Treatment of saline wastewater amended with endocrine disruptors by aerobic granular sludge: assessing performance and microbial community dynamics

Cyntia Ely[1*], Irina S. Moreira[2], João Paulo Bassin[1], Márcia W. C. Dezotti[1], Daniela P. Mesquita[3], Joana Costa[3], Eugénio C. Ferreira[3], Paula M. L. Castro[2]

[1]Universidade Federal do Rio de Janeiro, COPPE, Programa de Engenharia Química, Rio de Janeiro, Brazil

[2]Universidade Católica Portuguesa, Centro de Biotecnologia e Química Fina e Laboratório Associado, Escola Superior de Biotecnologia, Porto, Portugal

[3]Centre of Biological Engineering, Universidade do Minho, Campus de Gualtar, Braga, Portugal

* Corresponding author:

E-mail address: cyntia@peq.coppe.ufrj.br (Cyntia Ely).

Abstract

An aerobic granular sludge (AGS) sequencing batch reactor (SBR) adapted to salinity (12 g L^{-1} NaCl) was operated under alternating anaerobic-aerobic conditions for the treatment of synthetic saline wastewater containing endocrine-disrupting chemicals (EDCs), namely 17β–estradiol (E2), 17α–ethinylestradiol (EE2) and bisphenol-A (BPA). The SBR was intermittently fed with the EDCs at 2 mg L^{-1} of each compound. E2 was completely biodegraded, with 60% to 80% removal attained anaerobically and the remaining quickly consumed under aeration. EE2 was sorbed onto the granular sludge biomass in the anaerobic period, but it was desorbed in subsequent cycles even when the compound was not supplied to the reactor. BPA removal was poor but improved after bioaugmentation with an EDCs degrading bacteria. EDCs shock loads did not significantly affect the COD removal nor the activity of ammonium- and nitrite-oxidizing bacteria (AOB and NOB, respectively). In contrast, the activity of phosphate-accumulating organisms (PAOs) was affected, implying a decrease in P removal within the aerobic phase. AGS core microbiome grouped most bacteria belonging to the phylum Proteobacteria, followed by Bacteroidetes. The microbial profile showed that the introduction of the EDCs mixture increased the relative abundance of *Chryseobacterium* and *Flavobacterium*. AOB and NOB species were detected in the AGS biomass, with the latter showing lower relative abundance. Different PAOs, such as *Rhodocyclus*, *Tetrasphaera* and *Gemmatimonas*, were also part of the microbial community, but the addition of EDCs decreased significantly the relative abundance of *Rhodocyclus*. High microbial diversity was sustained over reactor operation, with the main bacterial groups responsible for nutrients and EDCs removal preserved in the AGS system. The results pointed to the maintenance of a core microbiome over reactor operation that may be related to the stability of the AGS process during EDCs loading.

Keywords: Aerobic granular sludge; Endocrine-disrupting chemicals; Saline wastewater; Nutrient removal; Microbial community: Bioaugmentation.

1 Introduction

Endocrine-disrupting chemicals (EDCs) are a kind of emerging contaminants that can disturb the normal hormone activities of humans and animals, causing adverse effects on their behaviour, growth, and immune function [1,2]. Pharmaceuticals and personal care products (PPCPs), hormones, industrial chemicals, surfactants, pesticides are some of the emerging contaminants [3]. Among the hormones commonly found in environmental matrices, 17β-estradiol (E2) and 17α-ethinylestradiol (EE2) stand out [4,5]. E2 is a natural estrogen crucial for the development and maintenance of female reproductive organs [6]. Livestock is one of the main sources of environmental contamination by E2 since this natural hormone is excreted by animals [7]. The excretion of E2 derived from pharmaceutical uses, including hormone replacement and treatment of some cancers, contributes only 5% to the overall contamination by this compound [8]. The exposure of aquatic organisms to E2 causes damage and health-related conditions [5]. On the other hand, 17α-ethinylestradiol (EE2) is a synthetic estrogen produced from the natural hormone E2. It is the main ingredient in most contraceptives and has other applications, such as interruption of breast milk production and hormone substitution [9]. EE2 has adverse ecological effects at concentrations lower than 4 ng/L [10]. The clearest sign has been observed in male fish exposed to estrogen (EE2-E2) impacted water bodies at 1–2 ng/L, presenting male and female sexual characteristics, such as partial evolution of eggs or ova [11].

Besides the natural and synthetic hormones, another important contaminant of water resources is the xenoestrogen bisphenol-A (BPA). Largely produced worldwide (about three million tons per year), its main use is to manufacture plastic and epoxy resins [12]. Even though BPA exhibits low estrogenic activity (10,000 to 100,000 times weaker than

that of E2) [13], it has been associated with serious health effects in humans and wildlife, causing several endocrine disorders [14].

E2, EE2 and BPA reach the environment due to inadequate disposal of non or partially treated domestic or industrial wastewater, the latter commonly associated with the inefficiency of wastewater treatment plants (WWTPs) [1,15,16]. For example, the conventional activated sludge (CAS) and membrane bioreactor (MBR) processes commonly implemented in WWTP appear to be unable to biodegrade these compounds completely, as some of them are toxic to microorganisms and resistant to microbial degradation [15,17]. Aerobic granular sludge (AGS) has been seen as a breakthrough in biological treatment, showing several properties that make it more attractive than CAS-based processes: higher compactness, capability of simultaneous removal of carbonaceous matter and nutrients in a single reactor, high shock load resistance, and excellent settling properties [18–20]. The latter is of utmost importance for allowing a good effluent clarification and high biomass retention within the bioreactor, characteristics attributed to the formation of regular and dense self-immobilized microbial clusters [18,21]. Such structure enables the development of many functional microbial groups acting in the biodegradation of refractory organic compounds [22]. Furthermore, the granular biomass layered structure leads to concentration gradients within the granule, protecting microorganisms from the toxicity associated with wastewater compounds [23]. AGS has also been shown to be a suitable biological process for the degradation of emerging contaminants of diverse nature [24–31]

Despite these key attractive features, the same challenges experienced in CAS reactors are also faced in AGS systems, especially concerning the removal of some specific micropollutants. Bioaugmentation, through the addition of specific single strains or microbial consortia, can enhance the biodegradation of target micropollutants [32], and

has been used in AGS systems for treating, for example, herbicides [33] and organofluorines [34,35]. However, most previous research addressing emerging contaminants removal by AGS were carried out in freshwater, while few studies on this topic were conducted under high salinity conditions [36,37]. Salinity is especially important in coastal cities where seawater is used as an alternative water source for toilet flushing [38,39]. As the microbial communities are often incapable of tolerating high osmotic pressures [40], the efficiency of the biological process may deteriorate when the wastewater treatment facilities receive saline wastewaters [41].

The objective of this study was to assess the ability of AGS to remove some emerging contaminants commonly detected in domestic wastewaters (i.e., E2, EE2 and BPA) under a saline environment (12 g L^{-1} NaCl). We hypothesised that bioaugmentation with a specific EDCs-degrading bacterial strain could improve the removal of such compounds and that the AGS could be set as an enrichment reactor for degrading strains. The contribution of adsorption and biodegradation mechanisms on the removal of the target compounds and their effects on reactor performance and AGS health were also addressed. The composition of the microbial community was assessed throughout the operation.

2 Materials and methods

2.1 Chemicals

E2, EE2, and BPA standards were acquired from Sigma Aldrich (purity > 98%) (Steinhein, Germany). HPLC grade methanol and acetonitrile were purchased from Merck (Darmstadt, Germany), while a Milli-Q water purification system provided ultra-pure water. Stock solutions of the EDCs mixtures were prepared at a concentration of

2,000 and 26,500 mg L^{-1} in methanol and stored at -20 °C in amber glass bottles. Analytical grade chemicals (Merck, Darmstadt, Germany; Sigma–Aldrich Chemie, Steinheim, Germany) were used to prepare the SBR influent synthetic wastewater [42].

2.2. AGS-SBR system

The experiment was conducted using a lab-scale AGS-SBR with 110 cm of total height, 6.5 cm of internal diameter and 2.5 L of a working volume. The system was operated in 3, 6, 8 and 12 h cycles. Automatic timers were employed to start and stop pumps during the reactor cycle. The cycles were divided into four consecutive phases: anaerobic feeding (60 min), when 0.95 L of influent was pumped into the reactor; aeration (112, 292, 412 and 645 min for the 3, 6, 8 and 12 h-cycles, respectively), during which compressed air was sparged into the reactor bottom at an airflow rate of 4 L min^{-1}; biomass settling (3 and 10 min) and effluent withdrawal (5 min). The reactor was operated at a volume exchange ratio of 39%. There was no control of the sludge retention time (SRT) throughout reactor operation; therefore, it was governed by natural suspended solids washout. The experiment was carried out with no oxygen and pH control. Nevertheless, their values remained fairly constant at 7.5 and 6 mg L^{-1} for pH and DO, respectively. The bioreactor was operated at room temperature (25 ± 2° C). The AGS biomass used as inoculum was taken from another lab-scale reactor that had been previously exposed to relatively high salinity (14 g L^{-1} NaCl). During the experiment, the salinity level was maintained under similar conditions.

2.3 Wastewater composition and operating conditions

The SBR influent wastewater was composed of two different solutions (A and B), as described by De Kreuk et al. [42]. Solution A comprised $NaCH_3COO$ $3H_2O$ (73.5 mM), $MgSO_4$ $7H_2O$ (3.6 mM) and KCl (4.7 mM), while solution B was composed of NH_4Cl (35.5 mM), Na_2HPO_4 (4.2 mM), KH_2PO_4 (2.2 mM) and NaCl (1 M). A trace element solution [43] was added to solution B (5 mL L^{-1}) to favour microorganisms growth. In each cycle, a volume of 89 mL of solution A and B was combined with 772 mL of water to achieve influent organic matter, ammonium and phosphate concentrations close to 450 mg L^{-1} (as COD), 50 mg NH_4^+-N L^{-1}, 16 mg PO_4^{3-}-P L^{-1}, respectively, a typical composition of domestic wastewater [44]. Small deviations from the desired values resulted from the influent preparation method and the mixing of solutions A and B by peristaltic pumps.

The bioreactor operation was divided into twelve experimental phases (Table 1). During phase I, acetate was the only carbon source present in the influent stream. From phase II (starting on the 14th day of reactor operation), a mixture of E2, EE2 and BPA was fed to the AGS-SBR. The mixture of EDCs was added to the influent during one cycle per day at the same cycle of the day. An appropriate quantity of the stock solution containing these compounds (2,000 mg L^{-1} of E2, EE2 and BPA, dissolved in methanol (phase II)) was added to solution A to reach an influent concentration of 2 mg L^{-1} of each compound. This concentration was set because of analytical limitations to detect and quantify them at the concentrations in which usually occur in environmental matrices, but above all, to allow a better investigation of removal mechanisms. In phase IV, a stock solution containing 26,500 mg L^{-1} of EDCs was prepared with the purpose of using a smaller amount of methanol, thus reducing its contribution to the influent COD. After this phase, the reactor had to be deactivated, and therefore, the biomass was stored under refrigeration at 4 °C for 60 days (this period has not been counted for the SBR operation

and occurred during the covid lockdown). The biomass was then reactivated for 17 days without the presence of EDCs (phase V).

For bioaugmentation of the SBR (phase VII) intended to improve the micropollutants removal efficiency, a previously isolated specialized strain of *Rhodococcus* sp. ED55, reported to be able to degrade EDCs [45], was used. ED55 pure cultures were placed in sealed flasks with a mineral salts medium and were incubated in an orbital shaker at a temperature of 25 °C and a rotating speed of 100 rpm. The optical density at 600 nm (OD600) was measured for microbial growth monitoring. The reactor was inoculated, respectively, with 20 mL and 11 mL of an ED55 pure culture with an OD600 of 0.614 and 0.810 after 20 and 28 min that the aerating period was started. During this period, the cycle time was increased 12 h, so the aeration and settling stages were extended to 652 min and 10 min, respectively. The duration of the other phases of the SBR remained invariant. This operating strategy was intended to maximize the permanence time of the strain within the reactor, preventing it from being washout with the effluent from the reactor.

During phase XI, the ammoniacal load was increased from 0.19 to 0.37 g d^{-1} m^{-3}. In the last regime (phase XII), the reactor returned to the initial imposed conditions (EDCs-free condition). The variation of influent COD and EDCs loads over the reactor operation associated with cycle time changes are displayed in Table 1.

2.4 Analytical methods

Samples routinely collected at the bioreactor influent stream, after the anaerobic feeding phase, and effluent were subjected to filtration in nylon membrane syringe filters (0.45 mm pore size) for biomass removal. EDCs (E2, EE2 and BPA) were analyzed using a

reversed-phase 250e4 HPLC-Cartridge LiChrospher 100 RP-18 column (Merck). The mobile phase comprised eluent A (water acidified at pH 2.2 with trifluoroacetic acid) and eluent B (acetonitrile). The elution started with 40% of eluent B for 4 min, followed by a gradient of 60% of eluent B (4 min) and 40% of eluent B (6 min), totalizing a run of 14 min at a constant flow rate of 0.8 mL min^{-1}. E2, EE2, and BPA retention time were 11.6, 12.1, and 10.0 min, respectively.

Spectroquant® (Merck Millipore) photometric test kits were used to measure COD, phosphate, ammonium, nitrite and nitrate concentrations in filtered samples, following the manufacturer's recommendations. Total and volatile suspended solids (TSS and VSS, respectively) were quantified following Standard Methods [46]. The AGS bed height was determined at the beginning of the feeding period through a ruler positioned over the reactor column.

Quantitative image analysis (QIA) was employed to observe morphological and physical characteristics of granules (the methodological procedure is detailed in the Supplementary Material). The extracellular polymeric substances (EPS) content was analyzed upon their extraction by a heat method, according to Felz et al. [47]. The carbohydrate content was measured through the anthrone-sulfuric acid method, using glucose as standard [48], while protein and humic acids contents were estimated by a modified Lowry method with bovine serum albumin as standard [49].

2.5 Isolation and identification of EDCs degrading strains from the SBR

Isolation of possible EDCs degrading strains was carried out by plating serial dilutions of crushed granules onto agar (LABM, UK), to which the SBR synthetic influent medium and 5 mg L^{-1} of each selected compound (E2, EE2, and BPA) were added. A volume of

100 µL of each dilution was spread onto the plates and incubated for 3 days at 25 °C. The bacterial colonies were isolated by means of the streak–plate procedure, taking into account the size, morphology, and pigmentation. After the growth of the isolated strains, they were incubated on an orbital shaker at 25 °C and 100 rpm to evaluate their E2, EE2, and BPA degradation capacity. Two 250 mL flasks containing 50 mL of SBR synthetic influent with 5 mg L^{-1} of each compound were tested. DNA extraction and sequencing analysis of the EDCs-degrading strains followed the description made by Duque et al.[34].

2.6 Microbial community analysis of AGS

2.6.1 DNA extraction

AGS samples were withdrawn from the bioreactor during the middle of aeration period at the end of some experimental phases. The genomic DNA extraction of aseptically crushed AGS samples was performed using the UltraClean Microbial DNA Isolation Kit (MoBio, USA), based on the manufacturer's protocol. The extracted DNA was kept at -20 °C until it was used for analysis.

2.6.2 Denaturing gradient gel electrophoresis (DGGE) analysis of PCR-amplified 16S rRNA

To amplify the variable V3 region of bacterial 16S rRNA gene fragments, primers 338F-GC and 518R were used [50]. The PCR reaction mixture and temperature profile were set as described by Amorim et al. [26]. The reactions were performed in a Bio-Rad iCycler

(Bio-Rad, USA). A DCode Universal Mutation Detection System (Bio-Rad, USA) (35% to 70% of denaturing gradient, with 100% denaturant defined as 7 M urea and 40% formamide) was used to separate PCR-amplified 16S rRNA gene fragments by DDGE. Electrophoresis was conducted in 1x TAE buffer at 60 °C and 20 V (the first 15 min) and 75 V (960 min). A 10x GelGreen Nucleic Acid Stain solution (Biotium Inc., USA) at 0.1 M NaCl concentration was used to stain the gels.

DGGE profiles were analysed employing Bionumerics software (Applied Maths, Belgium). Based on Pearson similarity coefficient with 1% tolerance, a dendrogram was elaborated and clustered with the unweighted pair group mean average (UPGMA) method. Shannon diversity index (H) [51] and equitability index (E) [52] were used to assess bacterial diversity and evenness of the microbial community, respectively.

2.6.3 Sequencing of DNA from DGGE bands and bioreactor biomass samples

A sterile scalpel was used to excise selected DGGE bands and eluted in 50 µL of sterile 10 mM Tris-HCl buffer (pH 8.00). After 48 h of incubation at 4 °C, the supernatant was re-amplified with the original primer set, which did not contain the GC clamp on the forward primer (338F). Illustra GFX^{TM} PCR DNA and Gel Band Purification Kit (GE Healthcare, USA), were used to purify PCR products. For identification and phylogenetic classification, band sequences were matched with the BLAST software from National Centre of Biotechnology Information website (http://www.ncbi.nlm.nih.gov/).

Next-generation sequencing (NGS) was performed using DNA from bioreactor biomass samples, without replicates. GATC-Eurofins (Konstanz, Germany) were used for all procedures, including amplificafion of DNA, preparation of libraries, sequencing and bioinformatic analysis. Two primers, covering the V3-V4 hypervariable region, (357F -

TACGGGAGGCAGCAG [53]; 800R - CCAGGGTATCTAATCC [54]) were used, and paired end sequencing based on 16S rRNA gene was conducted (Illumina MiSeq platform). Demultiplexing, clipping of primer sequences, merging, quality filtering and microbiome profiling integrated the steps of the microbiome analysis pipeline. To assign taxonomic information of the OTUs, DC-MEGABLAST alignments of cluster representative sequences were performed. Reference sequences with a minimum of 70% and 80% of identity and representative sequence, respectively, were selected and then processed with the QIIME software package (version 1.9.1, http://qiime.org/). The raw sequence data were deposited in Sequence Read Archive (SRA) from NCBI database, associated with the BioProject, under the accession number PRJNA645158.

3 Results and discussion

3.1 EDCs removal

Fig. 1 shows the average mass of each compound during the cycle subjected to shock load in the influent, after the anaerobic feeding phase, and effluent, while the concentrations throughout the operating days are presented in Fig. S1 (Supplementary Material).

In each cycle, the anaerobic period responded for the removal of 60% to 80% of E2, while the rest was quickly consumed in the aerated phase. E2 was no longer detected in the liquid phase after 10 min of aeration, as shown in the data from the cycle tests (Fig. S2). Biodegradation was assumed as the governing removal mechanism as the compound was removed from the bulk liquid and was never detected in the effluent. As reported in previous investigations, E2 exhibits high biodegradability. Fresh conventional activated sludge (CAS) oxidized E2 aerobically, reaching 1 mg L^{-1} and 1 µg L^{-1} after 1 and 3 h,

respectively [55], and a concentration of 5 to 15 µg L^{-1} was completely biodegraded in 2 h [56]. Kassotaki et al. [57] observed that E2 at 15 µg L^{-1} was always fully removed regardless of the conditions applied, whether by an enriched nitrifying activated sludge (NAS) and enriched AOB culture or by a CAS mixed bacterial consortia.

EE2 was initially removed in the anaerobic period within the shock period. This can be inferred because the concentration of EE2 after the anaerobic feeding period was lower than expected, considering its influent concentration and dilution in the reactor with the liquid remaining from the previous cycle (Fig. 1b). This removal was most probably attributed to EE2 adsorption onto the aerobic granules. However, this trend changed after phase VII, as the concentration after feeding was higher than that expected, implying a negative net removal under anaerobic conditions. This result is probably associated with the release of EE2 adsorbed in the granular biomass to the bulk liquid during the anaerobic feeding period. Indeed, results from the cycle tests (Fig S2) shows that EE2 concentration increased at the beginning of the aerated stage. The analyses performed in the subsequent cycles also suggest the desorption of EE2 from the granular biomass to the liquid because even after stopping the shock loads, EE2 was still detected in the effluent (Fig. S3a).

The total removal of EE2 became higher in phase VII (47%), when the reactor was bioaugmented with the specialized strain of *Rhodococcus* sp. ED55, and the HRT was set to 30.9 h. However, the removal dropped to 5.9% in phase VIII, even though the HRT was considerably higher (20.6 h) when compared to the initial phases (7.7 h). In phases X and XI, a negative EE2 removal efficiency was observed, implying that this compound was not removed from the system. A similar result was found by Moreira et al.[29] for fluoxetine, which was sorbed onto the biomass until saturation, after which desorption occurred, the latter being more evident in the periods of absence of fluoxetine. Kent and Tay [31] studied the removal of a mixture of EE2, 4-nonylphenol, and carbamazepine (all

at a concentration of 0.5 mg L^{-1}) from synthetic wastewater using AGS. Unlike what was observed in this research, the authors concluded that when the adsorption capacity saturated and biodegradation became the prevailing removal pathway, achieving removal efficiency of EE2 stabilized at an average of 77%. Also working with an AGS-SBR, Castellanos et al. [58] reported removal of 99% for E2 and 93% for EE2, both fed to the reactor at a concentration of 20 µg L^{-1}. In their study, profiles of E2 and EE2 over the reactor cycle suggested their rapid initial adsorption onto the granular biomass in the anaerobic period and biodegradation under aeration period. Maurício et al. [59] used synthetic and real wastewaters to examine the removal of 100 µg L^{-1} of E2 and EE2 in a rotating biological contactor (tertiary treatment stage). All assays showed removal efficiency above 50% for E2. The highest removals were observed for real wastewater. More than 15% reduction of EE2 concentrations was noticed in the tests using synthetic wastewater. Nevertheless, when real wastewater was employed, no removal was achieved. These authors also observed that EE2 was more hardly removed compared to E2. The recalcitrant behaviour of EE2 was expected since it is a synthetic hormone, proceeding from E2, with an ethynyl group at the C-17 position. The latter blocks access to the hydroxyl group situated in the same position, making the compound more difficult to be biodegraded [60].

Removal of BPA occurred in the anaerobic feeding and aerated period, starting from 33% and 5% during phase II, respectively. BPA biodegradation within the aerated period gradually improved, as indicated by the increase in removal to 51% at phase IV. Anaerobic removal increased around by 30% after bioaugmentation (phase VI), remaining stable until the end of the monitoring period. No BPA was detected in the effluent in phases with longer cycle times (12, 8, and 6 h). However, when the cycle time was reduced again to 3 h (phase X), BPA started again to be detected in effluent samples,

but at lower concentrations compared to the phases before the bioaugmentation. During phase XI, the overall removal increased to 95% (Table S1). The increasing BPA removal efficiency upon bioaugmentation suggests that biodegradation was the governing removal mechanism. This fact is more evident when phases II and X are compared, both with the operating cycle lasting 3 h (Fig S2). While in phase II BPA is still detected in the effluent samples, it reaches a concentration close to zero upon bioaugmentation, indicating that biodegradation was achieved. Fernandez et al. [61] reported a removal of 52–100% of BPA from sewage by activated sludge, and no adsorption or accumulation of such compound in the sludge was found. Moreover, adsorption of BPA on the biomass contributed only to 2–3% of the overall BPA abatement from domestic wastewater, with the remaining attributed to degradation [37].

Huang et al. [62] studied the sorption behaviour of targeted EDCs, including EE2 and BPA, onto activated sludge. Rapid sorption was observed in the first 15 min, within which 79.3% (for BPA) and 84.2% (for EE2) of the total sludge sorption capacity had been reached. The equilibrium was achieved after 5 h, at which 60.9% and 49.4% of EE2 and BPA were removed from the liquid phase. However, these compounds showed a high desorption potential, as 30–35% of the sorbed amount was dissolved back into the newly introduced wastewater.

Until now, there are still few reports on how saline wastewater interferes with the biological removal of EDCs. In particular, no previous work has addressed the removal of EDCs by AGS in saline wastewaters. The sorption of many organic pollutants onto suspended particles or sediments usually increases at higher salt concentrations due to the solubility of the hydrophobic compound that inversely depends on the dissolved salt concentration. This phenomenon is referred to as “salting-out effect” [63]. As a result of this effect, high salinity led to the transfer EDCs from the solution to particles and

sediments in an estuary located in China [64]. The increase in salt concentration also allowed E2 adsorption on granular activated carbon, chitin, chitosan, ion exchange resin, and a carbonaceous adsorbent [65]. Nevertheless, high salt concentration does not always favour adsorption. As observed by Xu et al. [66], BPA sorption on sediment increased with the salinity decrease.

3.2 COD, P and N removal

Within phase I, the AGS-SBR exhibited a stable COD removal efficiency, reaching effluent COD values of about 35 mg L^{-1} (Fig. 2a). Within the anaerobic feeding, almost all influent COD was consumed. In phase II, the EDCs mixture was incorporated into the influent wastewater, and, along with acetate, consisted of the feeding carbon sources. Methanol was used as a solvent for the EDCs stock solution containing 2,000 mg L^{-1} of these compounds. Under these conditions, a greater amount of methanol was fed to the reactor along with the EDCs and acetate, which increased the COD loading rate, reaching 1.4 kg m^{-3} d^{-1} (Table 1). Under anaerobiosis, i.e., in the absence of oxygen as a terminal electron acceptor, the selection of PAOs and GAOs is favoured [67]. These organisms can intracellularly accumulate storage polymers from volatile fatty acids, e.g., acetate, used as an energy source in the aerobic phase [68]. With the start of phase II, an appreciable amount of external substrate (acetate and methanol) became available in the aerated phase of the cycle, allowing its use by the fast-growing heterotrophic bacteria. This fact may have decreased the relative amount of PAOs and GAOs, and consequently, COD content in the bulk liquid after the anaerobic feeding and in the effluent increased up to 430 and 360 mg L^{-1}, respectively. Then, the EDCs were removed from the influent stream at phase III. In phase IV, the EDCs mixture returned to the reactor, but the influent

COD load was reduced to 1.0 kg m^{-3} d^{-1}. This was possible through the preparation of a more concentrated EDCs stock solution (26,500 mg L^{-1}), thus minimizing the interference of methanol on the incoming COD. Under these conditions, almost full COD abatement was observed during the anaerobic feeding period. The remaining COD in the effluent was due to the presence of non-biodegradable organic matter, partially present in the influent stream and partially derived from the by-products resulting from microbial degradation.

Concerning the phosphate concentration profiles, phosphorus content in the influent was maintained fairly constant throughout reactor operation (average 17 mgP L^{-1}) (Fig. 2b). Phosphate concentrations after the anaerobic feeding period were always higher than expected based on its influent concentration and dilution in the reactor, which reveals that PAOs released phosphate. However, P-release over time was very variable after phase II. A decline in phosphate consumption during the aerated phase was noticed in phase III and became even more pronounced in phase V (after the biomass has been stored at 4 °C for 60 days, which may have contributed to this result). After this period, phosphate uptake under aeration has not been fully restored, possibly associated with an inhibitory effect caused by EDCs on PAOs. The recovery of the phosphate removal was not observed even when the EDCs were removed from the reactor influent, demonstrating the sensitivity of the enhanced biological phosphorus removal process (EBPR) to the imposed conditions. The adverse effect of pharmaceutical compounds on biological phosphate removal was reported in previous studies [26,58]. Other studies observed that emerging contaminants led to a decrease in the anaerobic phosphate release, but the effluent phosphate concentrations were unaffected [27,31].

The presence of the EDCs mixture in the influent did not significantly affect ammonium removal (Fig. 2c), implying that the AGS structure could have protected AOB from the

presence of these compounds. In the first phase, ammonium was fully consumed. During phase II, a slight decrease in its removal (to around 96.7%) was observed upon EDCs supplementation. Nevertheless, it returned to 100% after interrupting the EDCs load (phase III), remaining so during phase IV. Shortly after the reactor reactivation (phase V), the effluent ammonium concentration reached more than 9 mgN L^{-1}, but AOB activity was recovered quickly, the effluent ammonium content dropped sharply and 100% removal was reached. Such performance was kept invariant throughout the next phases. The complete ammonium removal in the subsequent EDCs shock loads reinforces the great potential of aerobic granules in keeping stable nitrification in the presence of these compounds. Moreover, even when influent ammonium concentration was doubled (120 mgN L^{-1}) during phase XI, its removal only slightly decreased, showing the robustness of AGS system regarding nitrification. The increase in ammonium load was made to stimulate the development of nitrifying bacteria, as some authors suggest that these organisms are capable of improving the biodegradation of EDCs [69–72]. During this time, however, the removal of the EDCs, especially EE2, did not improve. However, it cannot be ignored that the time analysed under increasing ammonium load (phase XI) was relatively short (11 days only).

After anaerobic feeding and effluent throughout SBR operation, nitrite was observed at residual levels. Its maximum concentration in the effluent was approximately 1.6 mgN L^{-1} at phase V (Fig. 2e). Nitrate was the main nitrification product, being found in high concentrations in the effluent (Fig. 2d). Similar nitrate concentrations were observed during the phases without EDCs (I, III, and V), averaging 27 mgN L^{-1}. In addition to nitrification and denitrification processes, soluble nitrogen compounds (especially ammonium) were converted into bacterial biomass via assimilation (the calculation performed to estimate nitrogen consumption for growth purposes is described in

Supplementary Material – Equation S1). Assimilation for growth only accounted for 13% (on average) for the overall nitrogen removal. Nitrogen was mainly removed by denitrification (50.6% of TN removed by this process), except in phase VII, when assimilation (34.7%) was the main nitrogen removal route (Fig. S4).

In this study, NaCl concentration was kept constant at 12 g L^{-1}. Other researchers have previously investigated the sole effect of salt on COD, N and P removal by AGS during the treatment of saline wastewater. Paulo et al. [73] showed that variation in salt levels was not detrimental to any of these processes. The authors suggested that this result was possible due to the presence of EPS-producing bacteria. In the work of Li et al. [74], the performance of an AGS-SBR operating at relatively low salinity (1%) remained stable. However, at 2% and 4% salinity levels in terms of NaCl and K_2SO_4 (w/w = 1:1), the organic pollutants removal efficiencies deteriorated. P removal was impaired by salt concentrations above 21 g L^{-1} NaCl [75]. Other reports mentioned that the increase of salinity from 0 to 15 g L^{-1} led to significant drops in COD, N and P removal efficiency [40].

3.3 AGS characteristics

In this study, mature AGS with a light yellow color and a smooth and compact structure, and mean diameter of 1.15 mm, was used as inoculum in the SBR. Throughout the experiment period, the granules maintained such properties. The changes in biomass characteristics evaluated through image analysis are shown in Fig. S5. The granules were classified in IG (0.15 mm< D_{eq} <1.5 mm) and LG (D_{eq} >1.5 mm). Diameter (Fig. S5a) and granules average area (mm^2) (Fig. S5b) followed the same pattern over time. The same occurred for the relative amount (%) (Fig. S5c) of each class of granules. The total

number of granules varied according to the number of IG (0.15 mm< D_{eq} <1.5 mm), with the number of LG (D_{eq} ≥1.5 mm) remaining practically constant over the different operating phases (Fig. S5d). The morphological parameters, such as compactness (Fig. S5e) and robustness (Fig. S5f), remained practically constant over time.

Throughout the reactor operation, biomass was mostly composed of IG. However, a change in the size of the granular biomass from the inoculum (88% of IG) to phase II (71% of IG) occurred, remaining stable until phase V. This behaviour was not due to an increase in the amount of LG, but rather to a washout of IG, possibly due to biomass reactivation. When the EDCs feeding was restarted (phase VI), there was a slight decrease in D_{eq} of both IG and LG (from 0.778 ± 0.045 mm to 0.756 ± 0.018 mm and 1.915 ± 0.006 mm to 1.825 ± 0.070 mm, respectively). Concomitantly, the number of IG and LG increased and decreased, respectively, resulting in a reduction in the LG relative percentage, from 28% to 14%. The decrease in the relative amount of LG continued until it reached a minimum of 10% (phase IX). Moreover, in phase X, an increase in the D_{eq} of IG (from 0.757 ± 0.006 mm for 0.914 ± 0.026 mm) and the LG relative amount to 21% was noticed. This may be associated not only with the maturation of the granules, but also with the washout of the granules with lower D_{eq}.

Fig. 3a illustrates the solids content in the reactor over the operating time. The highest TSS values were observed during the first and last phases. In phase I, the mean TSS concentration was 15.5 g L^{-1}, with 63% corresponding to VSS, while in phase XII it amounted to 13 g L^{-1}, of which 86% was VSS (phase XII). The solids content gradually decreased until phase V, but increased after the restart period. At the beginning of bioaugmentation (phase VII), a cycle length of 12 h was used as an attempt to facilitate the retention of the bioaugmented bacterial strain inside the reactor. Under these conditions, an increment in the effluent TSS was observed (Fig. 3b). The longer aerated

phase may have caused the breakage of the granules due to more intense shear stress caused by aeration, leading to biomass loss during the settling and withdrawal phase. Other authors have also reported the adverse impact of long aeration periods on the granular biomass shape and size [29]. Sludge age was not controlled by manual sludge discharge, being therefore governed by natural solids washout (Fig. S6). During the first four phases, the SRT varied from 25 to 15 days. After the biomass storage period (phase V), the SRT dropped to 3 days due to biomass washout, but it gradually increased until the last operating phase. The food-to-microorganism ratio (F M^{-1}) was lower (0.04 gCOD $gVSS^{-1}$ d^{-1}) during the bioaugmentation period (phase VII) because of the longer aerated period (Fig. S6).

Closely associated with the stability of aerobic granules, EPS are usually the first barrier of bacterial cells that are in direct contact with the substrates, including toxic substances, therefore interacting with them (Wei et al., 2015). The EPS content of the AGS during the operating period is shown in Fig. S7. The concentrations of proteins (PN), polysaccharides (PS), and humic acids (HA), the main constituents of EPS, decreased from phase I to phase II and increased in phase IV. At the reactor restart (phase V), the concentrations of main EPS constituents decreased significantly when compared to the previous phase. In the following phases, their concentrations increased gradually. In phase VIII, a different profile was observed, with the PN content being greater than that of PS. In phase IX, the previous pattern was reestablished, but with a decrease in the overall EPS content. PN PS^{-1} ratio decreased gradually from phase I (1.94) to phase VI (0.85) and increased again in phase VII (1.06) until phase IX (1.27). Previous studies have been reported that the production of EPS was an important self-protection strategy of microorganisms against toxic substances. The latter may stimulate the production of exopolymers. Li et al. [28] reported that the toxicity of BPA (40 mg L^{-1}) played an

important role in the production of PN. On the other hand, Cydzik-Kwiatkowska et al. [30] found that EPS corresponded to around 20% of aerobic granules in the control reactor (no BPA) and only around 4-12% in the BPA-exposed granular biomass (2 to 12 mg L^{-1} BPA). Studies pointed out that high salinity tends to stimulate EPS secretion and, as a consequence, maintain good granular stability. Corsino et al. [76] have observed that EPS content increased under saline conditions compared to the control conditions without salt effect, while Hou et al. [77] noticed large variations between PN and PS contents under different salinity conditions in an AGS reactor. In another study, EPS analysis suggested that the improvement in metals adsorption of by AGS might have occurred due to increasing PS content after saline treatment (30 g L^{-1}) [78], suggesting that using salinity to increase EPS yield would be beneficial for adsorption. Sheng et al. [79] also pointed out that several organic pollutants can be adsorbed on the sludge because some hydrophobic regions in EPS are responsible for increasing the biomass adsorption capacity.

3.4 Identification of EDCs degrading strains

Using culture-dependent methods, twelve bacterial isolates were obtained from crushed granules, among which *Rhodococcus* ED55. According to BLAST results, seven strains were affiliated to Proteobacteria, one to Firmicutes and one to Actinobacteria phyla (Table 2). This result indicates that Proteobacteria played an important role in the degradation of EDCs. All of the bacterial isolates were closely related to isolates from environmental samples and shared similarities between 97% and 100% with the sequences deposited in GenBank. Previous studies suggest that are certain bacterial genera, e.g., *Rhodococcus*, *Pseudomonas*, or *Sphingopyxis*, that encompasses high

percentages of xenobiotic-degrading strains [80]. *Labrenzia aggregata* was isolated from East China Sea water samples, and *Brevibacillus halotolerans* was found to have a complex regulatory network that may help these bacteria adapt to complex environments under stressful conditions [81].

From the isolated bacterial strains, four of them were able to degrade E2 (Fig. 4a). Probably these organisms contributed to the degradation of E2 observed once this compound was added to the reactor influent wastewater. For all tests showing E2 degradation, E1 was generated and accumulated in the liquid medium (Fig.4b). However, the isolates were not capable of degrading E1 during the time course of the experiment. Yu et al. [82] indicated that only three strains of 14 isolates could degrade E1 within 7 days, after converting E2. Muller et al. [83] tested four isolates individually for estrogen removal, and only *Brevundimonas diminuta* could convert E2 to E1. For BPA, removals reached values of 22.7% and 21.8% with isolate *Rhodococcus ruber* and *Shewanella seohaensis*, respectively. While for EE2 there was no degradation. Considering the results from culture-dependent and -independent methods, it is likely the EDCs degradation by the AGS resulted from a syntrophic relationship between several isolates and non-isolated bacteria.

3.5 Microbial community of AGS

3.5.1 DGGE analysis

DGGE analysis of the 16S rRNA gene allowed tracking the changes in the bacterial community in biomass over the reactor operating phases. The DGGE banding profiles indicated a wide bacterial diversity (Fig. S8a). Most of the bands were present in almost

all samples, while others were only found in some sampling days. A band that apparently corresponds to *Rhodococcus* sp. can be seen on all lanes, suggesting that this bacterium was present in the biomass community since the reactor started operating, even before the bioaugmentation process. Unfortunately, it was not possible to excise the band and sequence it to confirm the identity because it was too thin.

Cluster analysis was carried out to assess the similarity between the DGGE profiles of each phase (Fig. S8b). The dendrogram showed that samples were classified into three main clusters. One of the main clusters was composed of the initial phases of operation of the reactor (I and II), the second one comprised phases III to VII (before bioaugmentation), and the third cluster was composed of phases VIII to XII. The first cluster, which includes phase I (no EDCs fed to the reactor), presented the lowest similarity between the other clusters (around 65%). This was probably associated with the EDCs, which induced changes in the granular biomass community in the subsequent phases.

The use of indices gives more information about the microbial community. Therefore, Shannon diversity index (H), used to evaluate the diversity of bacterial communities [51], and the Equitability index (E), which can range from 0 (no evenness) to 1 (complete evenness) [52] was calculated. H ranged from 1.27 (phase V) to 1.54 (phase XII) (Table S2). Nevertheless, no significant differences ($p>0.05$) were found in the community diversity. Concerning E, similar behaviour to the diversity index (0.82 to 1.06) was observed, with no significant differences over the reactor operating period ($p>0.05$)..

Seventeen different DGGE bands were excised for DNA sequencing (Fig. S8a), from which partial 16S rRNA gene sequences were successfully retrieved and compared with sequences from GenBank (Table S3). Most of the bacterial 16S rDNA sequences were classified as members of Proteobacteria. Band 18, whose intensity was very strong

compared to others, was present in all phases throughout reactor operation. The sequence corresponding to this band was closely associated with *Candidatus Accumulibacter*, commonly reported to be involved in P-removal.

3.5.2 Overall bacterial community within the AGS

From the 103 assigned OTUs, 82 were shared between samples from different experimental phases, accounting for around 90.8% of all sequences. From those OTUs, 44 OTUs were detected in all samples, representing about 42.7% of the total sequences. The core microbiome of the AGS was affiliated to Proteobacteria (27 OTUs, 61.8% of all sequences), Bacteroidetes (10 OTUs, 22.7% of all sequences), Actinobacteria (4 OTUs, 4.1% of the total sequences), Acidobacteria (1 OTU, 1.0% of all sequences) and Ignavibacteriae (1 OTU, 1.0% of all sequences) phyla.

The sequences results revealed that Proteobacteria were overabundant in all phases analysed, followed by Bacteroidetes (Fig. 5). Other phyla, such as Firmicutes, Gemmatimonadetes and Nitrospirae, showed a relative abundance lower than 0.5%. None of these were detected in all samples. Regarding class level, Betaproteobacteria was the most abundant (44.4%) in phase I (sample collected at day 1), whereas Gammaproteobacteria and Alphaproteobacteria become the predominant classes on day 77 within phase V (frequency of 23.3% and 21.5%, respectively) and on day 92, seven days after the bioaugmentation (phase VII) (frequency of 25% and 25.9%, respectively). Other class whose relative importance increased in these phases was Flavobacteriia, accounting for 17.2% (phase V) and 17.4% (Phase VII) of the total sequences, respectively. The bacterial distribution pattern in phase X was similar to that of phase I.

Rhodocyclaceae and *Xanthomonadaceae* were the most frequently detected families in the reactor, followed by *Flavobacteriaceae*, *Cytophagaceae*, *Chitinophagaceae* and *Caulobacteraceae*. Other families, e.g., *Actinobacteridae*, only appeared in lower abundance (Table S4).

As observed in previous studies addressing the microbial community of aerobic granules, members within Betaproteobacteria are predominant, including those closely associated with the families *Xanthomonadaceae*, *Comamonadaceae*, *Rhodoyclaceae* and *Nitrosomonadaceae*, all related to nitrification and denitrification processes [84]. From them, just *Nitrosomonadaceae* was not related to EPS production [85].

The heatmap with the evolution of the dominant bacterial genera in the AGS biomass (Table 3) shows that the frequency relative to some genera tended to increase or decrease with the addition of EDCs. Some strains were enriched in the reactor, such as those belonging to the genera *Chryseobacterium* and *Flavobacterium* within the Flavobacteriia class. For example, *Chryseobacterium*-like organisms increased from 3% (phase I) to around 12% (phase V and VII), becoming a dominant genus in AGS. However, over time, their abundance dropped to values initially found at the beginning of reactor operation (phase I). A similar trend happened with *Flavobacterium*, but with a lower relative abundance when compared to *Chryseobacterium*. Organisms associated with *Chryseobacterium* genus were found to play a key role in tetracycline removal [86], while *Flavobacterium* was dominant in AGS cultivated with pharmaceutical wastewater [87]. *Hyphomicrobium* and *Subsaxibacter*, although not detected in phase I, showed an increasing trend over time, with frequencies reaching 2.8% and 2.6%, respectively, in phase X. *Hyphomicrobium* was reported to contribute to a significant fraction (16%) of the bacterial community in an AGS system treating pharmaceutical compounds [88]. An increasing relative abundance was also observed for microorganisms belonging to the

genera *Mesorhizobium* and *Thiolamprovum*, likely due to their capability to adapt to the presence of EDCs.

The relative abundance of *Chryseolinea* genus decreased from 4.4% in phase I to 2.1% and 1.4% in phases V and VII, respectively, but increased to 2.9% in phase X. This behaviour may indicate that organisms within this genus were adversely affected by the EDCs mixture. However, the increase in the relative abundance suggests the adaptation of these organisms. *Rhodococcus* sp. was detected on day 92, eight days after bioaugmentation of the AGS system, and represented 0.4% of the total bacterial community. However, on day 120 (phase X), it was no longer observed in the bioreactor.

The sum of the relative abundance of the main genera associated with important functional groups within the AGS system is shown in Table S5. *Rhodocyclus* genus, closely associated with one of the main PAOs, predominated over other genera in phase I (37%). However, its relative frequency substantially decreased in subsequent phases to 9% (phase V) and 3% (phase VII), with a slight increase being observed in phase X (14%). This result was accompanied by a decline in phosphate consumption during the aerated phase from phase III, which became more pronounced in phase V. After this period, phosphate uptake under aeration has not been fully restored. Although at low relative abundance, other bacteria related to P-removal were observed during the reactor operation. *Tetrasphaera*-like organisms were detected in phases I, V and X, but not in phase VII. *Gemmatimonas*, also reported to be involved in P-removal [73], were present just in phases I and X, with a relative abundance of 0.5% and 0.4%, respectively.

Nitrifying bacteria were identified in all biomass samples (Table S5). The relative frequency of *Nitrosomonas*, a well-known AOB, gradually decreased from 3.8% (phase I) to 2.2% (phase V), 1.5% (phase VII) and 1.6% (phase X). Nevertheless, ammonium removal capacity was not adversely affected when the AGS reactor was exposed to the

EDCs load. The relative abundance of nitrite oxidizers of the genus *Nitrobacter* increased over time, from 0.3% (phase I) to 0.9% (phase X). It has been reported to be the dominant NOB in biological wastewater treatment systems [89]. *Nitrospira*, another nitrite oxidizer, was not identified only in phase I. NOB was present in lower relative abundance when compared to AOB. Despite their significant contribution to nitrogen turnover, the low relative abundance and diversity of nitrifying bacteria were already reported in previous studies [85]. The adverse impact of pharmaceuticals on nitrifying activity has also been reported, being the adverse effect more intense on NOB [87].

Denitrifying bacteria had the higher relative abundance among the bacterial functional groups in all phases analyzed, except during phase I (Table S5), indicating that this group was dominant and possibly relevant for the EDCs removal. *Denitromonas*, reported as dominant heterotrophic denitrifiers in aerobic granular biomass with a major role in denitrification under saline conditions [90], was also detected from phase V (0.5%) onwards. Its relative abundance increased over the experiment (0.8% and 1.4% for phases VII and X, respectively).

4 Conclusion

In this study, the effect of EDCs shock loading events on AGS-SBR performance and microbial community structure were assessed. E2 was efficiently biodegraded by the system, with 60% to 80% being converted anaerobically, and the remaining quickly consumed in the aerated phase. BPA was biodegraded after bioaugmentation with EDCs-degrading bacterial strain, while adsorption/desorption of EE2 onto aerobic granular biomass was found. EDCs shock loads did not significantly affect COD and ammonium removal, whereas phosphate removal was adversely affected. Nevertheless, AGS

structure may have protected the microbial community from the toxic effects of EDCs, leading to the maintenance of the carbon, nitrogen and phosphorus conversions. Molecular analyses showed that the presence of EDCs mixture led to dynamic changes in the microbial community profile, with increases in the relative abundance of *Chryseobacterium* and *Flavobacterium*. PAOs were severely affected by EDCs, corroborating the P removal performance results. Nevertheless, the results pointed to the presence of a core microbiome, which was maintained over reactor operation.

Supplementary Material

Additional Supplementary Material may be found in the online version of this article.

Figures captions

Fig. 1 Average mass of the E2 (a), EE2 (b) and BPA (c) during the cycle subjected to EDCs load. Legend: Influent (black bar), after anaerobic feeding – theoretical (medium grey bar) and measured mass (dark grey bar), effluent (light grey bar), anaerobic removal (●) and removal under aeration (○).

Fig. 2 COD (a), PO_4^{3-}-P (b), NH_4^+-N (c), NO_3^--N (d), and NO_2^--N (e) concentrations over the course of AGS-SBR operation. Legend: The roman numerals above the figures indicate the phases of operation. Concentrations in reactor influent (●), after anaerobic feeding (○) and effluent (▼) are shown.

Fig. 3 Solids content inside the reactor (a) and in the effluent (b). VSS TSS^{-1} ratio is also shown in (a). Legend: TSS (black bar), VSS (grey bar) and VSS TSS^{-1} ratio (○).

Fig. 4 E2 degradation by strains isolated from AGS (a) and E1 production (b). Legend: *Rhodococcus* sp. (E2 1) (●), *Brevundimonas* sp. (E2 2) (△), *Sphingopyxis* sp. (E2 3) (○), *Labrenzia* sp. (E2 4) (▼).

Fig. 5 Relative abundance of bacterial groups in class level with their respective phyla.

Acknowledgments

This study was supported in part by the Coordenação de Aperfeiçoamento de Pessoal de Nível Superior (CAPES/Brasil) – Finance Code 001 and the other part was financed by National Funds from Fundação para a Ciência e a Tecnologia (FCT/Portugal) - through the project AGeNT - PTDC/BTA-BTA/31264/2017 (POCI-01-0145-FEDER-031264) and the project CBQF - UID/Multi/50016/2019.

References

[1] T. Deblonde, C. Cossu-leguille, P. Hartemann, Emerging pollutants in wastewater: A review of the literature, Int. J. Hyg. Environ. Health. 214 (2015) 442–448. doi:10.1016/j.ijheh.2011.08.002.

[2] Y. Luo, W. Guo, H. Hao, L. Duc, F. Ibney, J. Zhang, S. Liang, X.C. Wang, A review on the occurrence of micropollutants in the aquatic environment and their fate and removal during wastewater treatment, Sci. Total Environ. 473–474 (2014) 619–641. doi:10.1016/j.scitotenv.2013.12.065.

[3] H. Chang, K. Choo, B. Lee, S. Choi, The methods of identification, analysis, and removal of endocrine disrupting compounds (EDCs) in water, J. Hazard. Mater. 172 (2009) 1–12. doi:10.1016/j.jhazmat.2009.06.135.

[4] M. Adeel, X. Song, Y. Wang, D. Francis, Y. Yang, Environmental impact of estrogens on human, animal and plant life: A critical review., Environ. Int. 99 (2017) 107–119. doi:10.1016/j.envint.2016.12.010.

[5] E. Nazari, F. Suja, Effects of 17β-estradiol (E2) on aqueous organisms and its treatment problem: a review, Rev. Environ. Health. 31 (2016) 465–491. doi:10.1515/reveh-2016-0040.

[6] L.L. Brunton, B.A. Chabner, B.C. Knollman, As bases farmacológicas da terapêutica de Goodman e Gilman, 10°, McGraw-Hill International Editions, 2005.

[7] M.C. Schuh, F.X.M. Casey, H. Hakk, T.M. DeSutter, K.G. Richards, E. Khan, P. Oduor, An on-farm survey of spatial and temporal stratifications of 17β-estradiol concentrations, Chemosphere. 82 (2011) 1683–1689. doi:10.1016/j.chemosphere.2010.10.093.

[8] T. de Mes, G. Zeeman, G. Lettinga, Occurrence and Fate of Estrone, 17β-estradiol and 17α-ethynylestradiol in STPs for Domestic Wastewater, Rev. Environ. Sci. Bio/Technology. 4 (2005) 275–311. doi:10.1007/s11157-005-3216-x.

[9] A.Z. Aris, A.S. Shamsuddin, S.M. Praveena, Occurrence of 17-α-ethynylestradiol

(EE2) in the environment and effect on exposed biota: a review, Environ. Int. 69 (2014) 104–119.

[10] K.A. Kidd, M.J. Paterson, M.D. Rennie, C.L. Podemski, D.L. Findlay, P.J. Blanchfield, K. Liber, Direct and indirect responses of a freshwater food web to a potent synthetic oestrogen, Philos. Trans. R. Soc. B Biol. Sci. 369 (2014). doi:10.1098/rstb.2013.0578.

[11] M. Woods, A. Kumar, Vitellogenin induction by 17β-estradiol and 17α-ethynylestradiol in male Murray rainbowfish (Melanotaenia fluviatilis), Environ. Toxicol. Chem. 30 (2011) 2620–2627. doi:10.1002/etc.660.

[12] L. Le Corre, P. Besnard, M.-C. Chagnon, BPA, an Energy Balance Disruptor, Crit. Rev. Food Sci. Nutr. 55 (2015) 769–777. doi:10.1080/10408398.2012.678421.

[13] W. V. Welshons, S.C. Nagel, F.S. vom Saal, Large Effects from Small Exposures. III. Endocrine Mechanisms Mediating Effects of Bisphenol A at Levels of Human Exposure, Endocrinology. 147 (2006) s56–s69. doi:10.1210/en.2005-1159.

[14] A. Shafei, M.M. Ramzy, A.I. Hegazy, A.K. Husseny, U.G. EL-hadary, M.M. Taha, A.A. Mosa, The molecular mechanisms of action of the endocrine disrupting chemical bisphenol A in the development of cancer, Gene. 647 (2018) 235–243. doi:10.1016/j.gene.2018.01.016.

[15] M. Boshir, J.L. Zhou, H. Hao, W. Guo, N.S. Thomaidis, J. Xu, Progress in the biological and chemical treatment technologies for emerging contaminant removal from wastewater: A critical review, J. Hazard. Mater. 323 (2017) 274–298. doi:10.1016/j.jhazmat.2016.04.045.

[16] Y.K.K. Koh, T.Y. Chiu, A. Boobis, E. Cartmell, M.D. Scrimshaw, J.N. Lester,

Treatment and removal strategies from wastewater, Environ. Technol. 29 (2008) 245–267.

[17] F.Y. Garcia-Becerra, I. Ortiz, Biodegradation of Emerging Organic Micropollutants in Nonconventional Biological Wastewater Treatment: A Critical Review, Environ. Eng. Sci. 35 (2018) 1–25. doi:10.1089/ees.2017.0287.

[18] J.. Beun, A. Hendriks, M.C.. van Loosdrecht, E. Morgenroth, P.. Wilderer, J.. Heijnen, Aerobic granulation in a sequencing batch reactor, Water Res. 33 (1999) 2283–2290. doi:10.1016/S0043-1354(98)00463-1.

[19] Y. Liu, J. Tay, State of the art of biogranulation technology for wastewater treatment, Biotechnol. Adv. 22 (2004) 533–563. doi:10.1016/j.biotechadv.2004.05.001.

[20] J.P. Bassin, Aerobic Granular Sludge Technology, in: Adv. Biol. Process. Wastewater Treat., Springer, Cham, 2018: pp. 75–148. doi:https://doi.org/10.1007/978-3-319-58835-3_4.

[21] S.S. Adav, D.-J. Lee, K.-Y. Show, J.-H. Tay, Aerobic granular sludge: Recent advances, Biotechnol. Adv. 237 (2008) 411–423. doi:10.1016/j.biotechadv.2008.05.002.

[22] F. Cai, L. Lei, Y. Li, Y. Chen, A review of aerobic granular sludge (AGS) treating recalcitrant wastewater: Refractory organics removal mechanism, application and prospect, Sci. Total Environ. 782 (2021) 146852. doi:10.1016/j.scitotenv.2021.146852.

[23] A.M. Maszenan, Y. Liu, W.J. Ng, Bioremediation of wastewaters with recalcitrant organic compounds and metals by aerobic granules, Biotechnol. Adv. 29 (2011) 111–123. doi:10.1016/j.biotechadv.2010.09.004.

[24] L. Balest, A. Lopez, G. Mascolo, C. Di Iaconi, Removal of endocrine disrupter compounds from municipal wastewater using an aerobic granular biomass reactor,

Biochem. Eng. J. 41 (2008) 288–294. doi:10.1016/j.bej.2008.05.015.

[25] X.H. Wang, V. Ivanov, Microbial structure of nitrifying granules and their estrogens degradation properties, Water Sci. Technol. 2 (2009) 1855–1863. doi:10.2166/wst.2009.218.

[26] C.L. Amorim, A.S. Maia, R.B.R. Mesquita, A.O.S.S. Rangel, M.C.M. van Loosdrecht, M.E. Tiritan, P.M.L. Castro, Performance of aerobic granular sludge in a sequencing batch bioreactor exposed to ofloxacin, norfloxacin and ciprofloxacin, Water Res. 50 (2014) 101–113. doi:10.1016/j.watres.2013.10.043.

[27] C.L. Amorim, I.S. Moreira, A.R. Ribeiro, L.H.M.L.M. Santos, C. Delerue-matos, M. Elizabeth, P.M.L. Castro, Treatment of a simulated wastewater amended with a chiral pharmaceuticals mixture by an aerobic granular sludge sequencing batch reactor, Int. Biodeterior. Biodegradation. 115 (2016) 277–285. doi:10.1016/j.ibiod.2016.09.009.

[28] K. Li, D. Wei, G. Zhang, L. Shi, Y. Wang, B. Wang, X. Wang, B. Du, Q. Wei, Toxicity of bisphenol A to aerobic granular sludge in sequencing batch reactors, J. Mol. Liq. 209 (2015) 284–288. doi:10.1016/j.molliq.2015.05.046.

[29] I.S. Moreira, C.L. Amorim, A.R. Ribeiro, R.B.R. Mesquita, A.O.S.S. Rangel, M.C.M. van Loosdrecht, M.E. Tiritan, P.M.L. Castro, Removal of fluoxetine and its effects in the performance of an aerobic granular sludge sequential batch reactor, J. Hazard. Mater. 287 (2015) 93–101. doi:10.1016/j.jhazmat.2015.01.020.

[30] A. Cydzik-Kwiatkowska, K. Bernat, M. Zielińska, K. Bułkowska, I. Wojnowska-Baryła, Aerobic granular sludge for bisphenol A (BPA) removal from wastewater, Int. Biodeterior. Biodegradation. 122 (2017) 1–11. doi:10.1016/j.ibiod.2017.04.008.

[31] J. Kent, J.H. Tay, Treatment of 17α-ethinylestradiol , 4-nonylphenol, and

carbamazepine in wastewater using an aerobic granular sludge sequencing batch reactor, Sci. Total Environ. 652 (2019) 1270–1278. doi:10.1016/j.scitotenv.2018.10.301.

[32] J. Benner, D.E. Helbling, H.E. Kohler, J. Wittebol, E. Kaiser, C. Prasse, T.A. Ternes, C.N. Albers, J. Aamand, B. Horemans, D. Springael, E. Walravens, N. Boon, Is biological treatment a viable alternative for micropollutant removal in drinking water treatment processes ?, Water Res. 47 (2013) 5955–5976. doi:10.1016/j.watres.2013.07.015.

[33] X. Quan, J. Ma, W. Xiong, X. Wang, Bioaugmentation of half-matured granular sludge with special microbial culture promoted establishment of 2,4-dichlorophenoxyacetic acid degrading aerobic granules, Bioprocess Biosyst. Eng. 38 (2015) 1081–1090. doi:10.1007/s00449-014-1350-y.

[34] A.F. Duque, V.S. Bessa, M.F. Carvalho, M.K. de Kreuk, M.C.M. van Loosdrecht, P.M.L. Castro, 2-Fluorophenol degradation by aerobic granular sludge in a sequencing batch reactor, Water Res. 45 (2011) 6745–6752. doi:10.1016/j.watres.2011.10.033.

[35] A.S. Oliveira, C.L. Amorim, J. Zlopasa, M. Van Loosdrecht, P.M.L. Castro, Recovered granular sludge extracellular polymeric substances as carrier for bioaugmentation of granular sludge reactor, Chemosphere. 275 (2021) 130037. doi:10.1016/j.chemosphere.2021.130037.

[36] S. Rózalska, P. Bernat, P. Michnicki, J. Długoński, Fungal transformation of 17α-ethinylestradiol in the presence of various concentrations of sodium chloride, Int. Biodeterior. Biodegrad. 103 (2015) 77–84. doi:10.1016/j.ibiod.2015.04.016.

[37] G.J. Zhou, X.Y. Li, K.M.Y. Leung, Retinoids and oestrogenic endocrine disrupting chemicals in saline sewage treatment plants: Removal efficiencies and

ecological risks to marine organisms, Environ. Int. 127 (2019) 103–113. doi:10.1016/j.envint.2019.03.030.

[38] G. Wu, Y. Guan, X. Zhan, Effect of salinity on the activity, settling and microbial community of activated sludge in sequencing batch reactors treating synthetic saline wastewater, Water Sci. Technol. 58 (2008) 351–358. doi:10.2166/wst.2008.675.

[39] D. Wu, G.A. Ekama, H. Chui, B. Wang, Y. Cui, T. Hao, M.C.M. Van Loosdrecht, G. Chen, Large-scale demonstration of the sulfate reduction autotrophic denitrification nitrification integrated (SANI ®) process in saline sewage treatment, Water Res. 100 (2016) 496–507. doi:10.1016/j.watres.2016.05.052.

[40] Z. Wang, M.C.M. Van Loosdrecht, P.E. Saikaly, Gradual adaptation to salt and dissolved oxygen : Strategies to minimize adverse effect of salinity on aerobic granular sludge, Water Res. 124 (2017) 702–712. doi:10.1016/j.watres.2017.08.026.

[41] Z. Li, T. Zhang, N. Li, X. Wang, Granulation of filamentous microorganisms in a sequencing batch reactor with saline wastewater, J. Environ. Sci. 22 (2010) 62–67. doi:10.1016/S1001-0742(09)60075-9.

[42] M.K. De Kreuk, J.J. Heijnen, M.C.M. Van Loosdrecht, Simultaneous COD, Nitrogen , and Phosphate Removal by Aerobic Granular Sludge, (2005). doi:10.1002/bit.20470.

[43] W. Vishniac, M. Santer, The Thiobacilli, Bacteriol. Rev. 21 (1957) 195–213.

[44] Metcalf and Eddy, Inc. Wastewater Engineering: Treatment, Disposal, Reuse, 1st ed., McGraw-Hill International Editions, New York, 1991.

[45] I.S. Moreira, A. Lebel, X. Peng, P.M.L. Castro, D. Gonçalves, Sediments in the mangrove areas contribute to the removal of endocrine disrupting chemicals in coastal

sediments of Macau SAR, China, and harbour microbial communities capable of degrading E2, EE2, BPA and BPS, Biodegradation. 9 (2021). doi:10.1007/s10532-021-09948-9.

[46] APHA, Standard Methods for the examination of water and wastewater, 21st ed., Washington, 2005. doi:ISBN 9780875532356.

[47] S. Felz, S. Al-Zuhairy, O.A. Aarstad, M.C.M. van Loosdrecht, Y.M. Lin, Extraction of Structural Extracellular Polymeric Substances from Aerobic Granular Sludge, J. Vis. Exp. 115 (2016) e54534.

[48] B. FROLUND*, R. PALMGREN, K. KEIDING, P.H.E. NIELSEN, Extraction of Extracellular Polymers From Activated Sludge Using A Cation Exchange Resin, Water Res. 30 (1996) 1749–1758.

[49] B. Frolund, T. Griebe, P.H. Nielsen, Enzymatic activity in the activated-sludge floc matrix, Appl. Microbiol. Biotechnol. 43 (1995) 755–761.

[50] G. Muyzer, E.C. Dewaal, A.G. Uitterlinden, Profiling of complex microbial populations by denaturing gradient gel electrophoresis of polymerase chain reaction-amplified genes coding for 16S rRNA, Appl. Environ. Microbiol. 59 (1993) 695–700.

[51] C.E. Shannon, W. Weaver, The Mathematical Theory of Communication, University of Illinois Press, Urbana and Chicago, 1963.

[52] E.C. PIELOU, Ecological Diversity, Wiley, New York, 1975, Joh Wiley and Sons, New York, 1975.

[53] S. Turner, K.M. Pryer, V.P.W. Miao, J.D. Palmer, Investigating deep phylogenetic relationships among cyanobacteria and plastids by small submit rRNA sequence analysis, J. Eukaryot. Microbiol. 46 (1999) 327–338.

doi:https://doi.org/10.1111/j.1550-7408.1999. tb04612.x.

[54] V. Kisand, R. Cuadros, J. Wikner, Phylogeny of culturable estuarine bacteria catabolizing riverine organic matter in the northern Baltic Sea, Appl. Environ. Microbiol. 68 (2002) 379–388. doi:https://doi.org/10.1128/aem.68.1.379-388.2002.

[55] T.. Ternes, M. Stumpf, J. Mueller, K. Haberer, R.-D. Wilken, M. Servos, Behavior and occurrence of estrogens in municipal sewage treatment plants — I. Investigations in Germany, Canada and Brazil, Sci. Total Environ. 225 (1999) 81–90. doi:10.1016/S0048-9697(98)00334-9.

[56] Q. Zeng, Y. Li, G. Gu, J. Zhao, C. Zhang, J. Luan, Sorption and biodegradation of 17β-estradiol by acclimated aerobic activated sludge and isolation of the bacterial strain, Environ. Eng. Sci. 26 (2009) 783–790. doi:10.1089/ees.2008.0116.

[57] E. Kassotaki, M. Pijuan, I. Rodriguez-Roda, G. Buttiglieri, Comparative assessment of endocrine disrupting compounds removal in heterotrophic and enriched nitrifying biomass, Chemosphere. 217 (2019) 659–668. doi:10.1016/j.chemosphere.2018.11.012.

[58] R.M. Castellanos, J.P. Bassin, D.M. Bila, M. Dezotti, Biodegradation of natural and synthetic endocrine-disrupting chemicals by aerobic granular sludge reactor: Evaluating estrogenic activity and estrogens fate, Environ. Pollut. 274 (2021) 1–10. doi:10.1016/j.envpol.2021.116551.

[59] R. Maurício, R. Dias, V. Ribeiro, S. Fernandes, A.C. Vicente, M.I. Pinto, J.P. Noronha, L. Amaral, P. Coelho, A.P. Mano, 17α-Ethinylestradiol and 17β-estradiol removal from a secondary urban wastewater using an RBC treatment system, Environ. Monit. Assess. 190 (2018). doi:10.1007/s10661-018-6701-8.

[60] L. Clouzot, M. Benoît, D. Pierre, N. Roche, 17α-ethinylestradiol: an endocrine disrupter of great concern. analytical methods and removal processes applied to water purification. A review., Environ. Prog. 27 (2008) 383–396.

[61] M.P. Fernandez, T.-N. Noguerol, S. Lacorte, I. Buchanan, B. Piña, Toxicity identification fractionation of environmental estrogens in waste water and sludge using gas and liquid chromatography coupled to mass spectrometry and recombinant yeast assay, Anal. Bioanal. Chem. 393 (2009) 957–968.

[62] Y. Huang, J. Guo, P. Yan, H. Gong, F. Fang, Sorption-desorption behavior of sulfamethoxazole, carbamazepine, bisphenol A and 17A-ethinylestradiol in sewage sludge, J. Hazard. Mater. 368 (2019) 739–745. doi:10.1016/j.jhazmat.2019.01.063.

[63] X. Shi, J.L. Zhou, H. Zhao, L. Hou, Y. Yang, Application of passive sampling in assessing the occurrence and risk of antibiotics and endocrine disrupting chemicals in the Yangtze Estuary, China, Chemosphere. 111 (2014) 344–351. doi:10.1016/j.chemosphere.2014.03.139.

[64] L. Yang, Q. Cheng, L. Lin, X. Wang, B. Chen, T. Luan, N.F.Y. Tam, Partitions and vertical profiles of 9 endocrine disrupting chemicals in an estuarine environment: Effect of tide, particle size and salinity, Environ. Pollut. 211 (2016) 58–66. doi:10.1016/j.envpol.2015.12.034.

[65] Y.P. Zhang, J.L. Zhou, Removal of estrone and 17b-estradiol from water by adsorption, Water Res. 39 (2005) 3991–4003.

[66] J. Xu, J. He, M. Wang, L. Li, Chemosphere Cultivation and stable operation of aerobic granular sludge at low temperature by sieving out the batt-like sludge, Chemosphere. 211 (2018) 1219–1227. doi:10.1016/j.chemosphere.2018.08.018.

[67] M.K. de Kreuk, M.C.M. van Loosdrecht, Selection of Slow Growing Organisms as a Means for Aerobic Granular Sludge Stability, Water Sci. Technol. 49 (2004) 9–17. doi:10.2166/wst.2004.0792.

[68] C.M. Lopez-Vazquez, C.M. Hooijmans, D. Brdjanovic, H.J. Gijzen, M.C.M. van Loosdrecht, Temperature effects on glycogen accumulating organisms, Water Res. 43 (2009) 2852–2864.

[69] A. Jantanaprasartporn, S. Maneerat, C. Rongsayamanont, Importance of culture history on 17α-ethinylestradiol cometabolism by nitrifying sludge, Environ. Eng. Res. 23 (2018) 28–35. doi:10.4491/eer.2017.044.

[70] J. Margot, S. Lochmatter, D.A. Barry, C. Holliger, Role of ammonia-oxidizing bacteria in micropollutant removal from wastewater with aerobic granular sludge, Water Sci. Technol. 73 (2016) 564–575. doi:10.2166/wst.2015.514.

[71] H. Roh, N. Subramanya, F. Zhao, C.-P. Yu, J. Sandt, K.-H. Chu, Biodegradation potential of wastewater micropollutants by ammonia-oxidizing bacteria, Chemosphere. 77 (2009) 1084–1089. doi:10.1016/j.chemosphere.2009.08.049.

[72] T. Yi, W.F. Harper, The link between nitrification and biotransformation of 17α-ethinylestradiol, Environ. Sci. Technol. 41 (2007) 4311–4316. doi:10.1021/es070102q.

[73] A.M.S. Paulo, C.L. Amorim, J. Costa, D.P. Mesquita, E.C. Ferreira, P.M.L. Castro, Long-term stability of a non-adapted aerobic granular sludge process treating fish canning wastewater associated to EPS producers in the core microbiome, Sci. Total Environ. 756 (2021) 144007. doi:10.1016/j.scitotenv.2020.144007.

[74] C. Li, W. Li, H. Li, M. Hou, X. Wu, The effect of quorum sensing on performance of salt- tolerance aerobic granular sludge: linking extracellular polymeric substances and

microbial community, Biodegradation. 30 (2019) 447–456. doi:10.1007/s10532-019-09886-7.

[75] M. Pronk, J.P. Bassin, M.K. De Kreuk, R. Kleerebezem, M.C.M. Van Loosdrecht, Evaluating the main and side effects of high salinity on aerobic granular sludge, Appl. Microbiol. Biotechnol. 98 (2014) 1339–1348. doi:10.1007/s00253-013-4912-z.

[76] S.F. Corsino, M. Capodici, C. Morici, M. Torregrossa, V. Gaspare, Simultaneous nitritation–denitritation for the treatment of high-strength nitrogen in hypersaline wastewater by aerobic granular sludge, Water Res. 88 (2016) 329–336.

[77] M. Hou, W. Li, H. Li, C. Li, X. Wu, Y. Liu, Performance and bacterial characteristics of aerobic granular sludge in response to alternating salinity, Int. Biodeterior. Biodegrad. 142 (2019) 211–217. doi:10.1016/j.ibiod.2019.05.007.

[78] X. Wu, W. Li, D. Ou, C. Li, M. Hou, H. Li, Y. Liu, Enhanced adsorption of Zn2+ by salinity-aided aerobic granular sludge: Performance and binding mechanism, J. Environ. Manage. 242 (2019) 266–271. doi:10.1016/j.jenvman.2019.04.094.

[79] G. Sheng, H. Yu, X. Li, Extracellular polymeric substances (EPS) of microbial aggregates in biological wastewater treatment systems : A review, Biotechnol. Adv. 28 (2010) 882–894. doi:10.1016/j.biotechadv.2010.08.001.

[80] A. Stolz, Molecular characteristics of xenobiotic-degrading sphingomonads, Appl. Microbiol. Biotechnol. 81 (2009) 793–811. doi:10.1007/s00253-008-1752-3.

[81] T. Xu, M. Yu, J. Liu, H. Lin, J. Liang, X.-H. Zhanga, Role of RpoN from Labrenzia aggregata LZB033 (Rhodobacteraceae) in Formation of Flagella and Biofilms, Motility, and Environmental Adaptation, Appl. Environ. Microbiol. 85 (2019) 1–12.

[82] C.P. Yu, H. Roh, K.H. Chu, 17B-Estradiol-Degrading Bacteria Isolated From

Activated Sludge, Environ. Sci. Technol. 41 (2007) 486–492. doi:10.1021/es060923f.

[83] M. Muller, D. Patureau, J.J. Godon, J.P. Delgenès, G. Hernandez-Raquet, Molecular and kinetic characterization of mixed cultures degrading natural and synthetic estrogens, Appl. Microbiol. Biotechnol. 85 (2010) 691–701. doi:10.1007/s00253-009-2160-z.

[84] S.S. Adav, D.J. Lee, J.Y. Lai, Microbial community ofacetate utilizing denitrifiers in aerobic granules, Appl. Microbiol. Biotechnol. 85 (2010) 753–762. doi:https://doi.org/10.1007/s00253-009-2263-6.

[85] E. Szabó, R. Liébana, M. Hermansson, O. Modin, F. Persson, W.J. Hickey, D.G. Weissbrodt, Microbial Population Dynamics and Ecosystem Functions of Anoxic/Aerobic Granular Sludge in Sequencing Batch Reactors Operated at Different Organic Loading Rates, Front. Microbiol. 8 (2017) 1–14. doi:10.3389/fmicb.2017.00770.

[86] X. Wang, Z. Chen, J. Kang, X. Zhao, J. Shen, Removal of tetracycline by aerobic granular sludge and its bacterial community dynamics in SBR, RSC Adv. 8 (2018) 18284–18293. doi:10.1039/c8ra01357h.

[87] C.L. Amorim, M. Alves, P.M.L. Castro, I. Henriques, Bacterial community dynamics within an aerobic granular sludge reactor treating wastewater loaded with pharmaceuticals, Ecotoxicol. Environ. Saf. 147 (2018) 905–912. doi:10.1016/j.ecoenv.2017.09.060.

[88] B. Muñoz-palazon, A. Rosa-masegosa, M. Hurtado-martinez, A. Rodriguez-sanchez, A. Link, R. Vilchez-vargas, A. Gonzalez-martinez, J.G. Lopez, Aerobic Granular Sludge Systems Operated in Sequential Batch Reactors: Effect of Pharmaceutical Compounds, Toxics. 93 (2021) 1–20.

[89] J.R. Vázquez-Padín, M. Figueroa, A. Mosquera-Corral, J.L. Campos, R. Méndez, Population dynamics of nitrite oxidizers in nitrifying granules, Water Sci. Technol. 60 (2009) 2529–2536.

[90] J. Yao, W. Li, D. Ou, L. Lei, M. Asif, Y. Liu, Performance and granular characteristics of salt-tolerant aerobic granular reactors response to multiple hypersaline wastewater, Chemosphere. 265 (2021) 129170. doi:10.1016/j.chemosphere.2020.129170.

Fig. 1

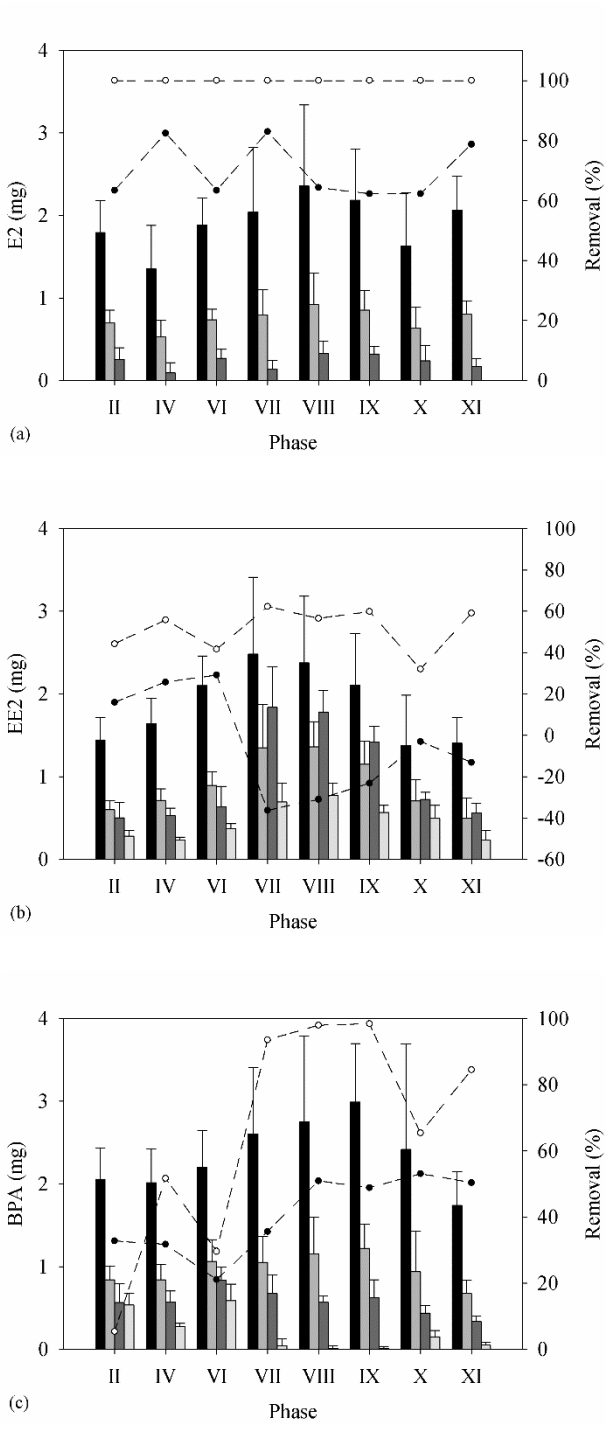
E2 (mg)
Removal (%)
Phase
II
IV
VI
VII
VIII
IX
X
XI
(a)
EE2 (mg)
Removal (%)
Phase
(b)
BPA (mg)
Removal (%)
Phase
(c)

Fig. 2

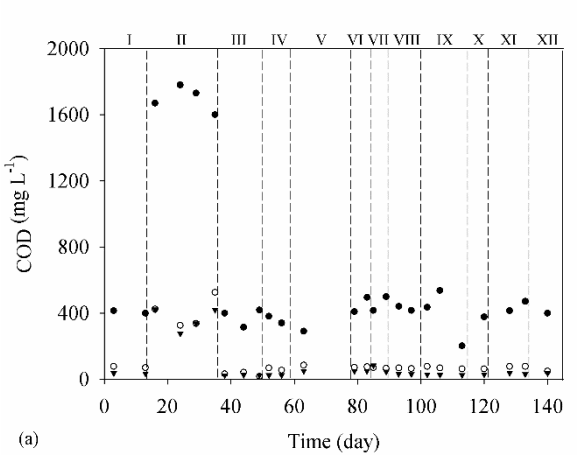
I II III IV V VI VII VIII IX X XI XII
COD (mg L-1)
Time (day)
(a)

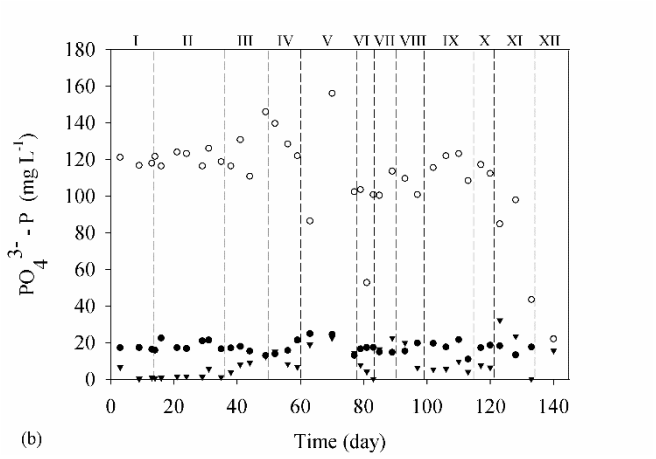
I II III IV V VI VII VIII IX X XI XII
PO4 3- - P (mg L-1)
Time (day)
(b)

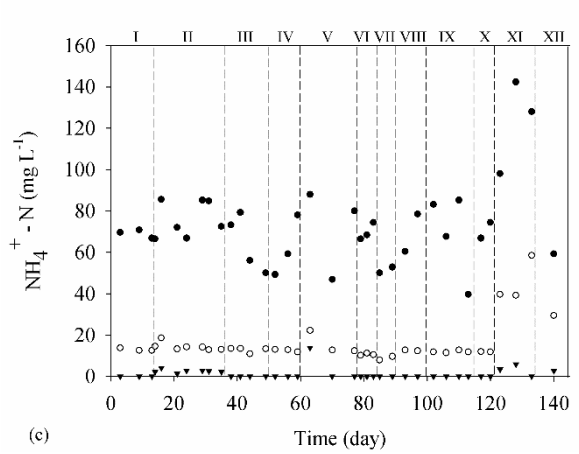
I II III IV V VI VII VIII IX X XI XII
NH4 + - N (mg L-1)
Time (day)
(c)

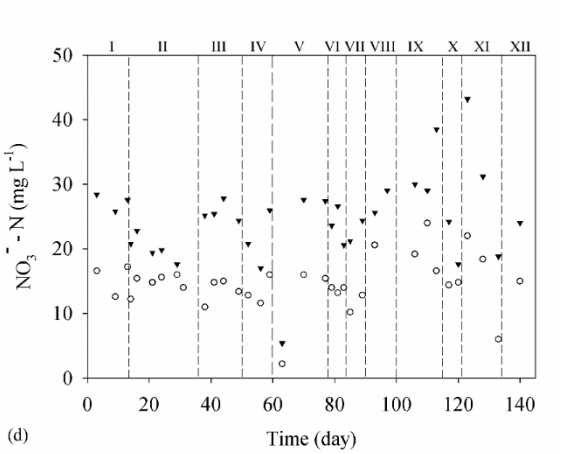
I II III IV V VI VII VIII IX X XI XII
NO3 - - N (mg L-1)
Time (day)
(d)

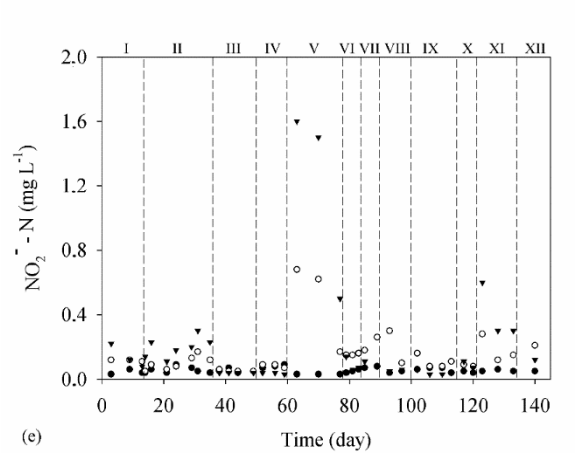
I
II
III
IV
V
VI
VII
VIII
IX
X
XI
XII
2.0
1.6
1.2
0.8
0.4
0.0
NO_2^- - N (mg L^{-1})
0
20
40
60
80
100
120
140
Time (day)
(e)

Fig. 3

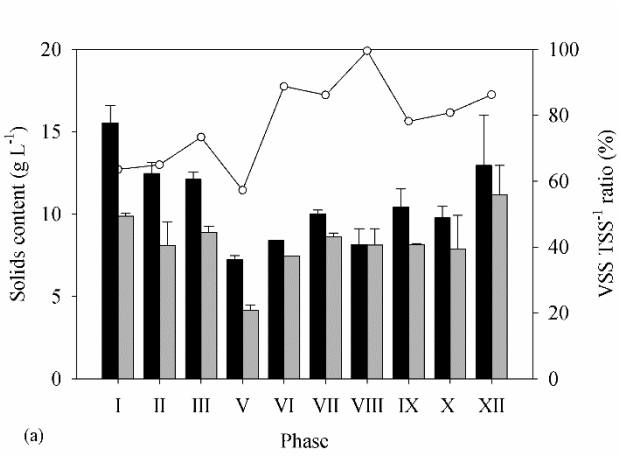
20
15
10
5
0
Solids content (g L^{-1})
100
80
60
40
20
0
VSS TSS^{-1} ratio (%)
I
II
III
V
VI
VII
VIII
IX
X
XII
Phase
(a)

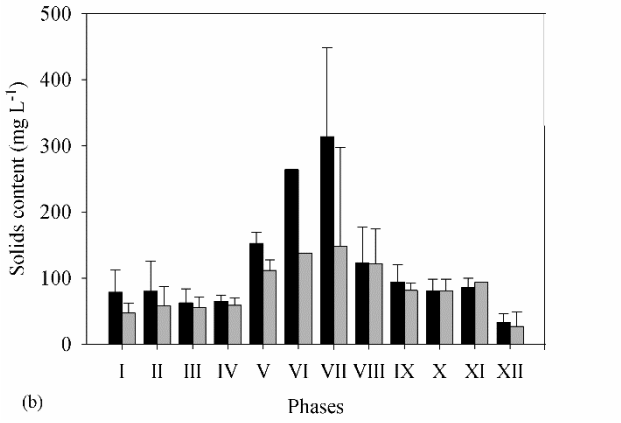
500
400
300
200
100
0
Solids content (mg L^{-1})
I
II
III
IV
V
VI
VII
VIII
IX
X
XI
XII
Phases
(b)

Fig. 4

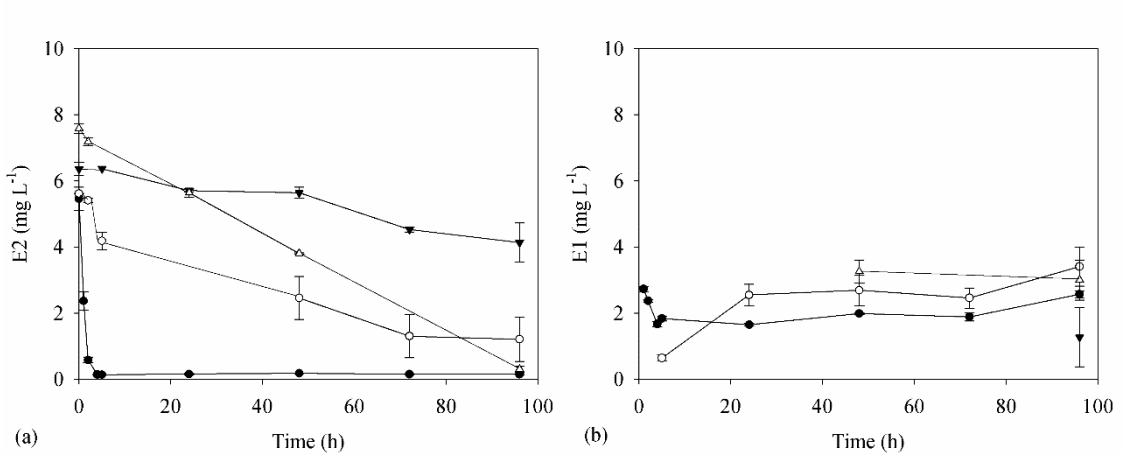
E2 (mg L-1)
E1 (mg L-1)
Time (h)
Time (h)
(a)
(b)

Fig. 5

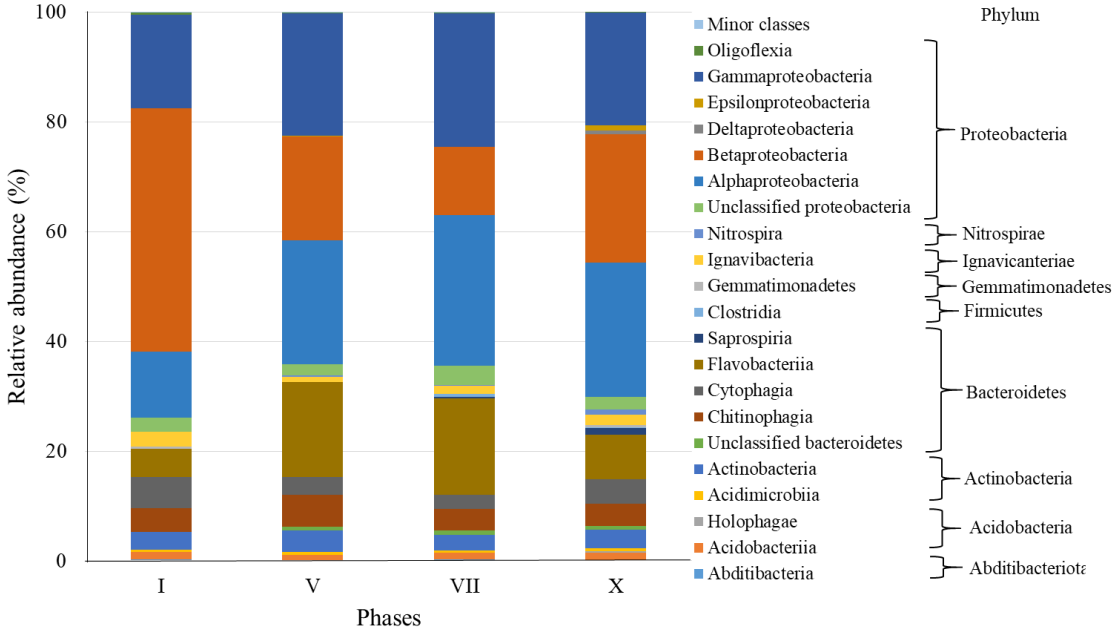
Relative abundance (%)
Phases
I
V
VII
X
Minor classes
Oligoflexia
Gammaproteobacteria
Epsilonproteobacteria
Deltaproteobacteria
Betaproteobacteria
Alphaproteobacteria
Unclassified proteobacteria
Nitrospira
Ignavibacteria
Gemmatimonadetes
Clostridia
Saprospiriia
Flavobacteriia
Cytophagia
Chitinophagia
Unclassified bacteroidetes
Actinobacteria
Acidimicrobiia
Holophagae
Acidobacteriia
Abditibacteria
Phylum
Proteobacteria
Nitrospirae
Ignavicanteriae
Gemmatimonadetes
Firmicutes
Bacteroidetes
Actinobacteria
Acidobacteria
Abditibacteriot

Table 1 Operating conditions tested over the SBR operation.

Phase	SBR operating conditions								
	Operation length (days)	Cycle time (h)	Influent feeding (min)	Aeration (min)	Settling (min)	Effluent withdrawal (min)	HRT (h)	Influent COD load (kg m^{-3} d^{-1})	Influent EDCs load (mg m^{-3} d^{-1})
I	1 – 13	3	60	112	3	5	7.7	1.0	0
II	14 – 37	3	60	112	3	5	7.7	1.4	18.6
III	38 – 49	3	60	112	3	5	7.7	1.0	0
IV	50 – 59	3	60	112	3	5	7.7	1.0	18.6
V	60 – 77	3	60	112	3	5	7.7	1.0	0
VI	78 – 83	3	60	112	3	5	7.7	1.0	18.6
VII	84 – 92	12	60	645	10	5	30.9	0.3	4.6
VIII	93 – 99	8	60	412	3	5	20.6	0.4	7.0
IX	100 – 113	6	60	292	3	5	15.5	0.5	9.3
X	114 – 120	3	60	112	3	5	7.7	1.0	18.6
XI	121–132	3	60	112	3	5	7.7	1.0	18.6
XII	133 – 140	3	60	112	3	5	7.7	1.0	0

Table 2 Phylogenetic affiliation of bacterial isolates extracted from the biomass.

Isolate	Closest relative	Phylogenetic affiliation	Similarity (%)	Accession n°	Compound biodegradation (%)
E2 1[a]	*Rhodococcus ruber* strain DSM 43338	Actinobacteria	99.7	NR_026185.1	100
E2 2	*Brevundimonas diminuta* strain NBRC 12697	α-proteobacteria	99.8	NR_113602.1	96
E2 3[b]	*Sphingopyxis terrae* strain NBRC 15098	α-proteobacteria	99.8	NR_113727.1	80
E2 4	*Labrenzia aggregata* strain NBRC 16684	α-proteobacteria	97.1	NR_113861.1	35
E2 5	*Pseudomonas composti* strain C2	γ-proteobacteria	99.8	NR_116992.1	No
EE2 1	*Acinetobacter johnsonii* strain ATCC 17909	γ-proteobacteria	99.8	NR_117624.1	No
EE2 2	*Pseudomonas plecoglossicida* strain FPC951	γ-proteobacteria	99.7	NR_024662.1	No
EE2 3[b]	*Sphingopyxis terrae* strain NBRC 15098	α-proteobacteria	99.8	NR_113727.1	No
EE2 4	*Brevibacillus halotolerans* strain LAM0312	Bacilli	96.9	NR_156834.1	No
BPA 1[a]	*Rhodococcus ruber* strain DSM 43338	Actinobacteria	99.9	NR_026185.1	22.7
BPA 2	*Shewanella seohaensis* strain S7-3	γ-proteobacteria	99.8	NR_108852.1	21.8
BPA 3	*Paracoccus huijuniae* strain FLN-7	α-proteobacteria	97.8	NR_108224.1	No

[a, b] The strains with the same letters are equals.

Table 3 Heatmap presenting the evolution in dominant genera in the AGS biomass. Only the more abundant bacterial genera were considered in this analysis.

Genus	Phase			
	I	V	VII	X
Rhodocyclus	37.7	9.5	3.1	14.2
Lysobacter	9.8	7.9	8.7	7.1
Chryseobacterium	2.9	12.3	12.1	3.3
Brevundimonas	2.8	6.7	8.2	4.2
Edaphocola	4.3	5.9	3.7	3.9
Azoarcus	0.8	4.9	2.8	3.6
Chryseolinea	4.4	2.1	1.4	2.9
Frigoribacterium	2.3	2.7	2.4	2.5
Mesorhizobium	0.9	2.3	2.5	3.5
Paracoccus	0.6	3.4	3.4	1.9
Nitrosomonas	3.8	2.2	1.5	1.6
Thiolamprovum	0.2	2.1	2.7	3.5
Pseudofulvimonas	2.0	2.1	2.1	2.7
Hydrogenophaga	1.8	0.8	3.3	1.7
Flavobacterium	0.9	2.7	2.6	0.9
Defluviicoccus	2.3	1.8	1.0	1.8
Ignavibacterium	2.7	0.8	1.2	1.8
Candidatus Solibacter	1.4	0.9	1.2	1.3
Mariniflexile	0.8	1.6	1.6	0.8
Hyphomicrobium	0.0	0.5	1.3	2.8
Subsaxibacter	0.0	0.5	1.3	2.6
Rhodobacter	0.7	1.3	0.9	1.1
Erythrobacter	0.0	0.0	1.2	1.6
Denitromonas	0.0	0.5	0.9	1.3
Tetrasphaera	0.5	1.1	0.0	0.9
Nitrobacter	0.3	0.5	0.4	0.9
Nitrospira	0.0	0.3	0.2	1.1

0 to 1
1 to 2.5
2.5 to 5
5 to 10
10 to 20
20 to 100

Supplementary Material

Treatment of saline wastewater amended with endocrine disruptors by aerobic granular sludge: assessing performance and microbial community dynamics

Cyntia Ely[1], Irina S. Moreira[2], João Paulo Bassin[1], Márcia W. C. Dezotti[1], Daniela P. Mesquita[3], Joana Costa[3], Eugénio C. Ferreira[3], Paula M. L. Castro[2]

[1]Universidade Federal do Rio de Janeiro, COPPE, Programa de Engenharia Química, Rio de Janeiro, Brazil

[2]Universidade Católica Portuguesa, Centro de Biotecnologia e Química Fina e Laboratório Associado, Escola Superior de Biotecnologia, Porto, Portugal

[3]Centre of Biological Engineering, Universidade do Minho, Campus de Gualtar, Braga, Portugal

Quantitative image analysis procedure

Duplicate AGS biomass samples were collected during the middle of the aeration period over the reactor operation, washed with phosphate-buffered saline (PBS) solution, and incubated in a mixture of PBS and formaldehyde 4% (0.25:1) for 2 h at 4 °C. Then, the biomass was washed with PBS and preserved in a solution of PBS and ethanol 96% (1:1). The granules were transferred to a Petri dish for visualization and image acquisition through an Olympus magnifying glass, with a total magnification of 15x. The granules were classified into two classes based on their equivalent diameter (D_{eq}): IG – Intermediate-sized granules (0.15 mm< D_{eq} <1.5 mm), and LG – Large-sized granules (D_{eq} ≥1.5 mm). The acquired images were processed using the Matlab program (The Mathworks, Inc., Natick), as described by Ramos et al. (2017).

Assimilation of nitrogen

The amount of incorporated ammonium nitrogen (gN d^{-1}) for cell growth was estimated according to the modified equation (Wan et al., 2009):

$$N_{assimilated} = f_N \times VSS_{effluent} \times O \qquad \text{(Equation S1)}$$

Where f_N is the fraction of nitrogen in the sludge (0.12389 mgN $mgVSS^{-1}$); O is the output (L d^{-1}); $VSS_{effluent}$ is the concentration of solids in the final effluent (gVSS L^{-1}).

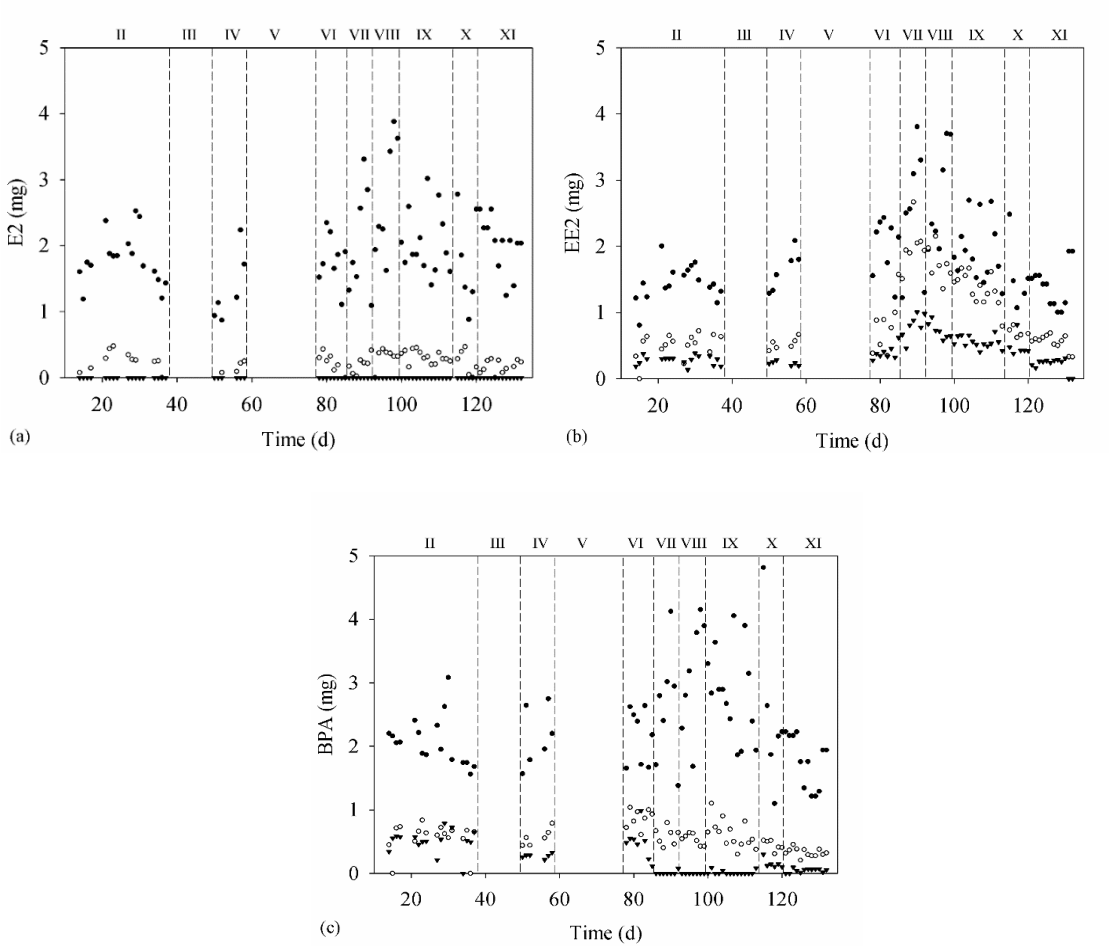

Fig. S1 EDCs concentration in the cycle with the shock load: (a) E2, (b) EE2, and (c) BPA. Symbols: (●) influent, (○) after anaerobic period, (▼) effluent concentration. These compounds were not added to the influent stream in phases III and V.

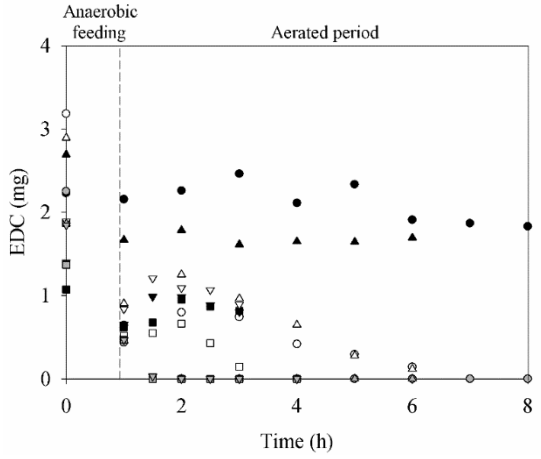

Fig. S2 EDCs mass profiles during a typical shock load cycle: E2 (grey), EE2 (black), and BPA (white). Symbols: Phases II – 3 h-cycle (square), VIII – 8 h-cycle (circle), IX – 6 h-cycle (triangle up) and X – 3 h-cycle (triangle down).

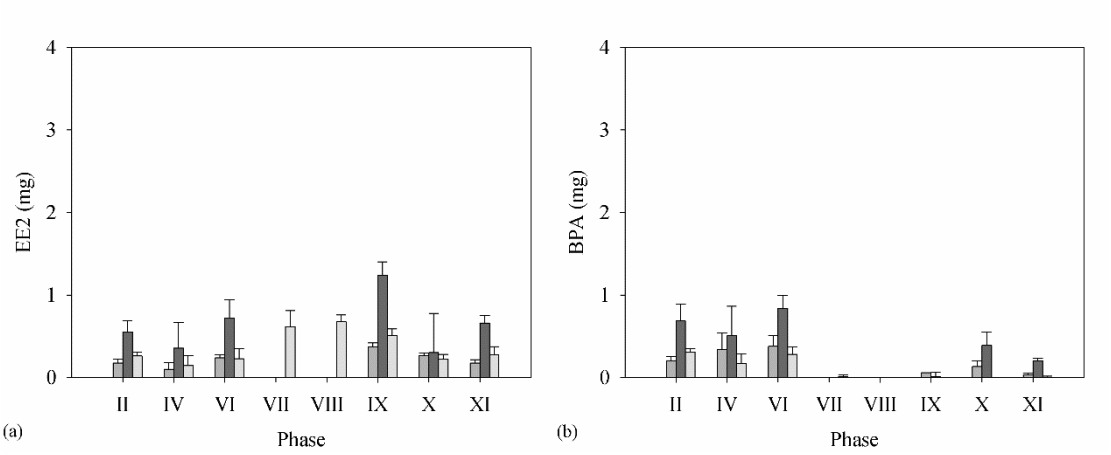

Fig. S3 Average mass of EE2 (a) and BPA (b) during the first cycle without EDCs. Legend: After anaerobic feeding – theoretical (medium grey bar) and measured mass (dark grey bar), effluent (light grey bar).

Table S1 EDCs mass balance during the shock load cycles. The mass of each compound in the effluent considers all daily cycles within a given phase.

Phase	Compound	Influent (mg d^{-1})	Effluent (mg d^{-1})	Removal (%)
II	E2	1.8 ± 0.4	<0.1	100
	EE2	1.4 ± 0.3	1.3 ± 0.4	12.5
	BPA	2.0 ± 0.4	1.2 ± 0.6	41.0
IV	E2	1.3 ± 0.5	<0.1	100
	EE2	1.6 ± 0.3	1.1 ± 0.3	32.9
	BPA	2.0 ± 0.4	1.1 ± 0.5	45.7
VI	E2	1.9 ± 0.3	<0.1	100
	EE2	2.1 ± 0.4	1.3 ± 0.3	35.7
	BPA	2.2 ± 0.4	1.9 ± 0.2	14.1
VII	E2	2.0 ± 0.8	<0.1	100
	EE2	2.5 ± 0.9	1.3 ± 0.4	47.2
	BPA	2.6 ± 0.8	0.1 ± 0.5	96.9
VIII	E2	2.4 ± 1.0	<0.1	100
	EE2	2.4 ± 0.8	2.2 ± 0.4	5.9
	BPA	2.7 ± 1.0	0.01 ± 0.03	99.6
IX	E2	2.2 ± 0.6	<0.1	100
	EE2	2.1 ± 0.6	2.0 ± 0.3	5.2
	BPA	3.0 ± 0.7	0.01 ± 0.03	99.7
X	E2	1.6 ± 0.6	<0.1	100
	EE2	1.4 ± 0.6	1.4 ± 0.1	-4.3
	BPA	2.1 ± 1.3	0.1 ± 0.1	93.2
XI	E2	2.1 ± 0.4	<0.1	100
	EE2	1.4 ± 0.3	1.6 ± 0.4	-12.8
	BPA	1.7 ± 0.4	0.1 ± 0.05	95.4

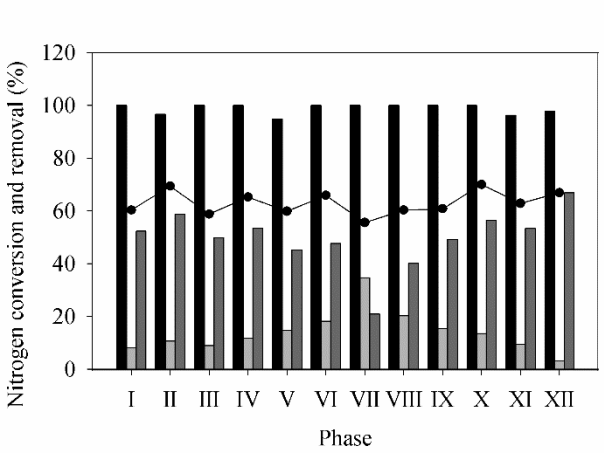

Fig. S4 Nitrogen removal by bacterial assimilation and denitrification. Legend: Ammonium converted into nitrite/nitrate by nitrification (black bar), nitrogen assimilation (light grey bar), denitrification (dark grey bar) and total nitrogen removal (•).

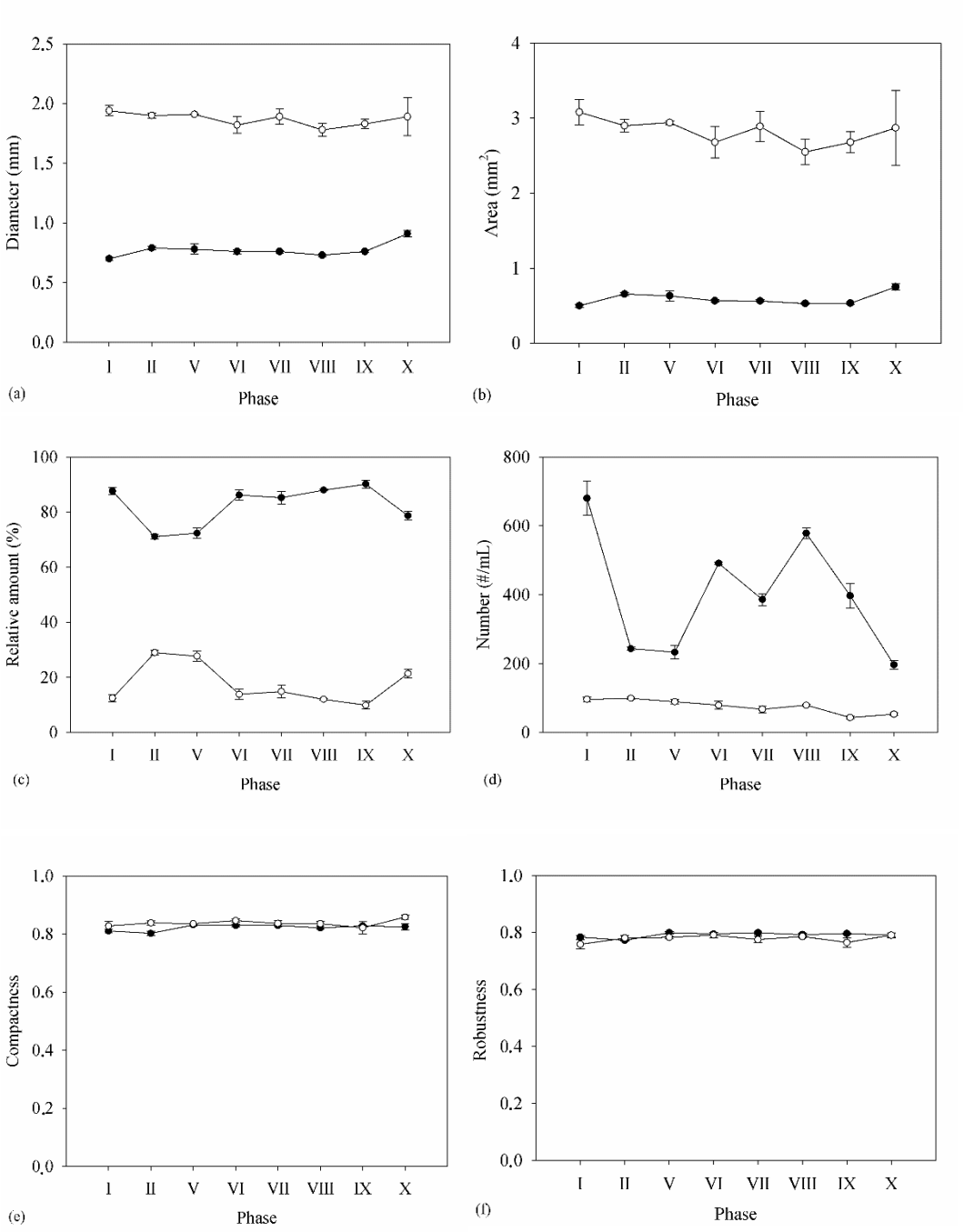

Fig. S5 Granules average equivalent diameter (a), area (b), relative amount (c), number of granules (d), compactness (e) and robustness (f) for large-sized (○) and intermediate-sized granules (•) throughout reactor operation.

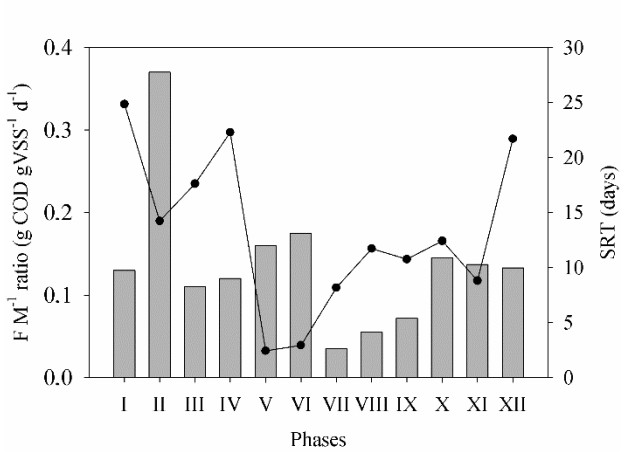

Fig. S6 Food-to-microorganism ratio (grey bar) and SRT (•).

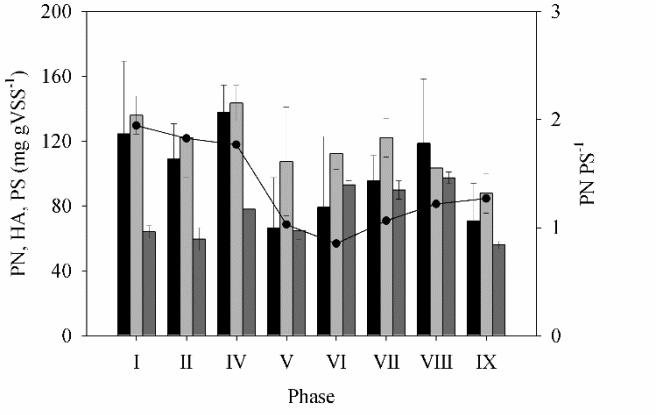

Fig. S7 Proteins (black bar), humic acids (medium grey bar), polysaccharides (dark grey bar), and PN PS^{-1} (•).

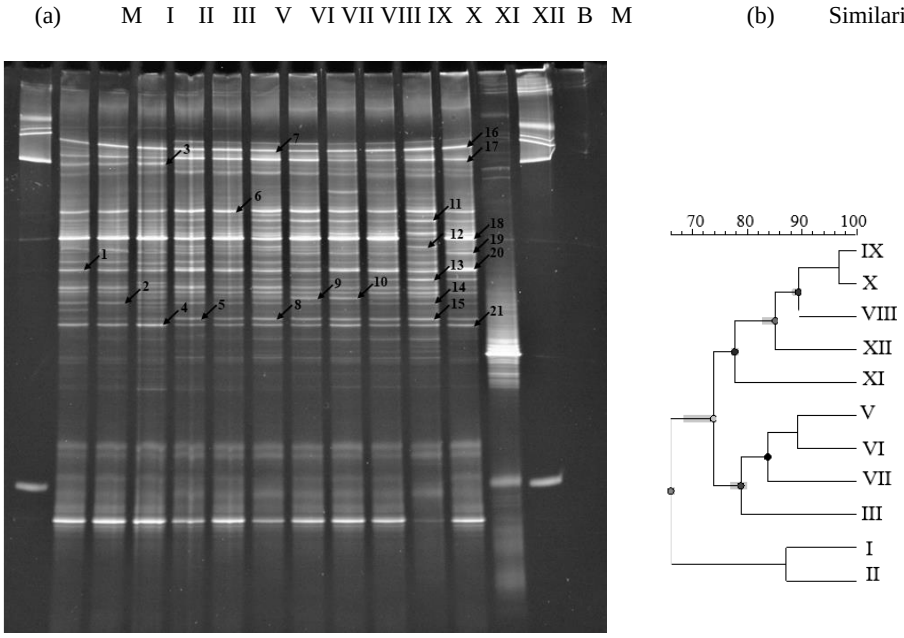

Fig. S8 DGGE analysis of 16S rRNA fragments of total bacterial community within the aerobic granules. (a) DGGE fingerprint of the SBR bacterial community. Different gel lanes correspond to samples collected during SBR operation (phases are indicated on the top of the lanes). Lane M: DNA marker; Lane B: EDCs degrading bacterial strain. (b) UPGMA cluster analysis of bacterial communities based on DGGE profile. Dendrogram presents the similarity, in percentage, between the DGGE samples. Similarities were calculated using the Jaccard measure.

Table S2 Shannon diversity (H) and Equitability (E) indexes

Phase	H	E
I	1.38	0.96
II	1.41	0.96
III	1.30	0.84
V	1.27	0.82
VI	1.29	0.83
VII	1.34	0.88
VIII	1.37	0.91
IX	1.42	0.95
X	1.43	0.97
XI	1.34	0.87
XII	1.54	1.06

Table S3 Phylogenetic affiliation of DGGE band DNA sequences.

Band n°.	**Phylogenetic affiliation**	**Closest relative (accession n°.)**	**Similarity (%)**	**Isolation source**
1 and 2	γ-proteobacteria	*Lysobacter* sp. strain CHu50b-3-2 (MK696268.1)	96	Sediments
3	β-proteobacteria	Uncultured Nitrosomonadales bacterium AOBseq_3b (HQ455817.1)	88	Water from ornamental fish transporting system
4 and 21	Unknown	Uncultured bacterium clone MA00070D11 (FJ772390.1)	94	Huron River /host zebra mussels
5	Chloroflexi	Uncultured Anaerolineae (AB752317.1)	88	In situ colonization system deployed in a Japanese shallow hydrothermal vent
6	γ-proteobacteria	*Luteimonas* sp. strain BO171 (MK201763.1)	89	-
7	Unknown	Uncultured bacterium isolate DGGE gel band BUJIT2 (GQ245699.1)	89	Landfill leachate
8	Chloroflexi	Uncultured Chloroflexi bacterium clone IAFpp7125 (GU214133.1)	87	Slime sample from a papermaking mill taken at the wet section around a papermaking machine
9	Unknown	Uncultured bacterium (LN875367.1)	91	Primary sludge from a tannery wastewater treatment plant
10	β-proteobacteria	*Janthinobacterium lividum* strain K5 (KP775922.1)	94	Vaginal swab /host Homo sapiens
11	Unknown	Uncultured bacterium clone OTU_61 (MN194806.1)	96	Barley (Hordeum vulgare) rhizosphere
12, 18 and 19	β-proteobacteria	Uncultured *Candidatus Accumulibacter* sp. clone 38 (JQ726367.1)	98	Sequencing batch reactor for P removal

Table S3 Phylogenetic affiliation of DGGE band DNA sequences (continuation)

13	Bacteroidetes	Uncultured Flavobacteriaceae (AB543529.1)	83	Sewage treatment plant
14	α-proteobacteria	*Paracoccus* sp. strain JL3606 (KX989148.1)	94	Shallow-sea hydrothermal system in Kueishantao Islet
15	Chloroflexi	Uncultured Chloroflexi bacterium clone Pink_2B07 (GQ483921.1)	95	Intertidal thrombolites
16	Unknown	Uncultured bacterium clone OTU_6613 (KX974029.1)	96	Tropical urban freshwater
17	Bacteroidetes	Uncultured *Cloacibacterium* sp. CSVI076 (MG552002.1)	81	Biofilm
20	β-proteobacteria	*Azoarcus* sp. strain HKLI-1 (MN493120.1)	97	Sewage

Table S4 Heatmap presenting the evolution in dominant bacterial families in the AGS biomass. Only the more abundant bacterial families were considered in this analysis.

	Phases			
Family	I	V	VII	X
Rhodocyclaceae	37.69	10.05	3.98	15.52
Xanthomonadaceae	14.26	17.59	18.96	13.43
Flavobacteriaceae	4.65	17.15	17.55	7.63
Caulobacteraceae	2.79	6.72	8.21	4.22
Chitinophagaceae	4.32	5.90	3.99	4.09
Rhodobacteraceae	2.77	5.78	5.30	4.28
Zoogloeaceae	0.81	4.90	2.80	3.79
Fulvivirgaceae	4.88	2.35	1.60	3.44
Phyllobacteriaceae	1.65	3.16	3.34	4.22
Sphingomonadaceae	1.13	3.41	4.71	2.32
Rhodanobacteraceae	2.41	2.55	2.48	3.19
Microbacteriaceae	2.26	2.73	2.40	2.53
Nitrosomonadaceae	3.77	2.22	1.55	1.64
Comamonadaceae	2.06	1.11	3.70	2.07
Chromatiaceae	0.22	2.06	2.69	3.49
Rhodospirillaceae	2.97	1.86	1.16	2.15
Ignavibacteriaceae	2.69	0.83	1.23	1.84
Erythrobacteraceae	0.00	0.00	2.15	2.79
Hyphomicrobiaceae	0.00	0.55	1.39	2.82
Solibacteraceae	1.44	0.88	1.17	1.29

0 to 1
1 to 2.5
2.5 to 5
5 to 10
10 to 20
20 to 100

Table S5 Relative abundance (%) of the main genera associated with important functional groups within the AGS system. The sum of each category is shown in bold.

		Phases			
Functional group	Genus	I	V	VII	X
PAO	*Rhodocyclus*	37.7	9.5	3.1	14.2
	Tetrasphaera	0.5	1.1	0.0	0.9
		38.2	**10.6**	**3.1**	**15.1**
GAO	*Defluviicoccus*	2.3	1.8	1.0	1.8
Nitrifying bacteria	*Nitrosomonas*	3.8	2.2	1.5	1.6
	Nitrobacter	0.3	0.5	0.4	0.9
	Nitrospira	0.0	0.3	0.2	1.1
		6.4	**4.8**	**2.1**	**3.6**
Denitrifying bacteria	*Lysobacter*	9.8	7.9	8.7	7.1
	Hydrogenophaga	1.8	0.8	3.3	1.7
	Azoarcus	0.8	4.9	2.8	3.6
	Mesorhizobium	0.9	2.3	2.5	3.5
	Paracoccus	0.6	3.4	3.4	1.9
	Flavobacterium	0.9	2.7	2.6	0.9
	Rhodobacter	0.7	1.3	0.9	1.1
	Denitromonas	0.0	0.5	0.9	1.3
		14.9	**23.8**	**25.1**	**21.1**